

# Fourier-based solvers for diffusion & wave propagation phenomena

Faisal Amlani

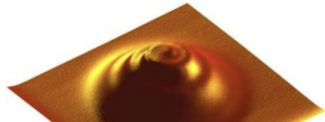
CNRS *Chargé de Recherche* (Research Fellow / Permanent Faculty)

Laboratoire de Mécanique Paris-Saclay (LMPS)

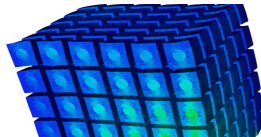
Université Paris-Saclay

# A little bit about our laboratory

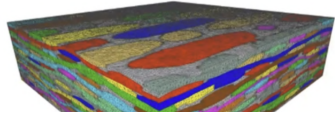
- est. 2022 as a fusion of LMT (ENS Paris-Saclay) & MSSMat (CentraleSupélec)
- many partners (including Safran, EDF, CEA, Airbus, RATP, Michelin, etc.)
- ~220 members (including ~57 permanent researchers & ~90 PhD students)



**COMMET**: COmportement des Matériaux,  
Modélisation, Expérimentation et Théorie



**STAN**: Science et Techniques Avancées  
en mécanique Numérique



**MILA**: MILieux Architecturés



**OMEIR**: Ouvrages, Matériaux,  
Environnement : Interactions et Risques

# A little bit about me



🇺🇸 Austin  
*grade school (K-12)*



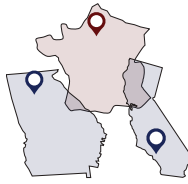
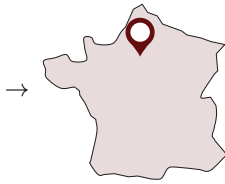
🇺🇸 Houston  
*BA, applied math*



🇺🇸 Pasadena  
*PhD, applied math*



🇺🇸 Los Angeles  
*aero R&D startup*



🇫🇷 Paris  
*postdoc (math/acoustics)*



🇺🇸 Los Angeles  
*postdoc (fluid-structure)*



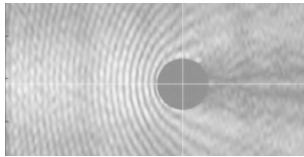
🇫🇷 Paris  
*tenured researcher*

# Towards explaining observations in the lab or nature

Controlled **experimental** data

→ Coarse **natural** data

Ultrasonic material testing



$\mathcal{O}(\text{microseconds})$

Pulsatile blood flow



$\mathcal{O}(\text{milliseconds})$

Seismogenic tsunamis



$\mathcal{O}(\text{seconds})$

## Applied Mathematics

- ▶ **targeted methods**
- ▶ idealized configurations
- ▶ theoretical verifications



## Computational Mechanics

- ▶ general methods
- ▶ **realistic configurations**
- ▶ **experimental validations**

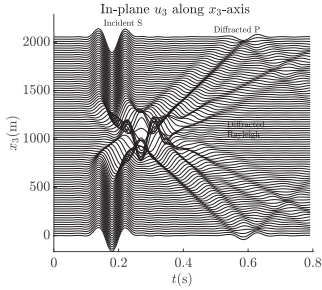
# Time-dependent PDEs for continuum problems

(classic linear examples)

Hyperbolic systems (e.g., wave-like)

$$\frac{\partial^2 u(\mathbf{x}, t)}{\partial t^2} = c^2 \nabla^2 u(\mathbf{x}, t)$$

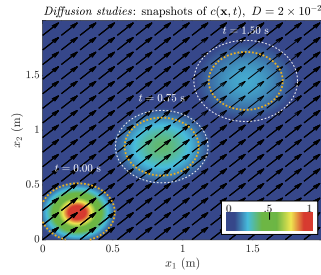
- ▶ advection/convection phenomena
- ▶ disturbances propagate at finite speed (which can be nonlinear)



Parabolic systems (e.g., heat-like)

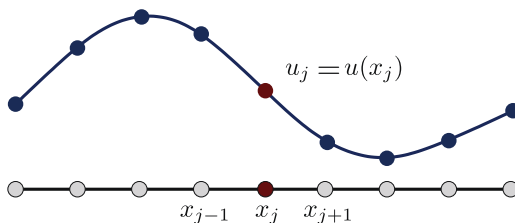
$$\frac{\partial \phi(\mathbf{x}, t)}{\partial t} = D \nabla^2 \phi(\mathbf{x}, t)$$

- ▶ conduction/diffusion phenomena
- ▶ disturbances felt essentially all at once (similarly to elliptic)



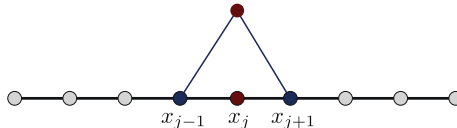
# Brief review of spectral methods

► goal: high-order spatial differentiation



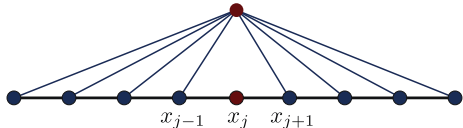
Local methods (e.g., FD/FE/FV)

Global methods



$$\text{error} = \mathcal{O}(\Delta x^p)$$

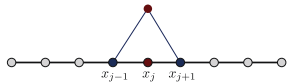
$(p = 1, 2, 3, \dots \text{fixed})$



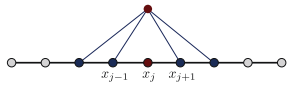
$$\text{error} = \mathcal{O}(\Delta x^{1/\Delta x})$$

(if  $u \in C^\infty$ , else  $\mathcal{O}(\Delta x^p)$  for  $u \in C^p, u \notin C^{p+1}$ )

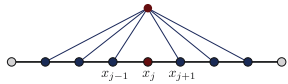
# Brief review of spectral methods



$$\mathcal{O}(\Delta x^2) : u_x(x_j) \approx \frac{u_{j+1} - u_{j-1}}{2\Delta x}$$



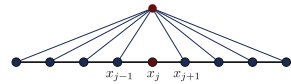
$$\mathcal{O}(\Delta x^4) : u_x(x_j) \approx \frac{-u_{j+2} + 8u_{j+1} - 8u_{j-1} + u_{j-2}}{12\Delta x}$$



$$\mathcal{O}(\Delta x^6) : u_x(x_j) \approx \frac{u_{j+3} - 9u_{j+2} + 45u_{j+1} - 45u_{j-1} + 9u_{j-2} - u_{j-3}}{60\Delta x}$$

⋮

⋮



$$\begin{aligned} \mathcal{O}(\Delta x^N) : u_x(x_j) \approx & \quad \frac{1}{2} \cot\left(\frac{\Delta x}{2}\right) (u_{j+1} - u_{j-1}) - \\ & - \frac{1}{2} \cot\left(\frac{2\Delta x}{2}\right) (u_{j+2} - u_{j-2}) + \\ & + \frac{1}{2} \cot\left(\frac{3\Delta x}{2}\right) (u_{j+3} - u_{j-3}) - \dots \end{aligned}$$

$$(N \rightarrow \infty : u_x(x_j) \approx \frac{1}{h}(u_{j+1} - u_{j-1}) - \frac{1}{2h}(u_{j+2} - u_{j-2}) + \dots)$$

# Brief review of spectral methods

- ▶ example: FD operator for five-point stencil

$$\begin{pmatrix} u_x(x_1) \\ \vdots \\ u_x(x_N) \end{pmatrix} = \begin{pmatrix} 0 & \frac{2}{3} & -\frac{1}{12} & & \frac{1}{12} & -\frac{2}{3} \\ -\frac{2}{3} & \ddots & \ddots & \ddots & & \frac{1}{12} \\ \frac{1}{12} & \ddots & \ddots & \ddots & & \\ & \ddots & \ddots & \ddots & \ddots & \\ & & \ddots & \ddots & \ddots & -\frac{1}{12} \\ -\frac{1}{12} & \frac{2}{3} & -\frac{1}{12} & & \frac{1}{12} & -\frac{2}{3} & 0 \end{pmatrix} \begin{pmatrix} u(x_1) \\ \vdots \\ u(x_N) \end{pmatrix}$$

- ▶ banded sparse matrix  $\implies \sim \mathcal{O}(N)$  operations

## Brief review of spectral methods

► example:  $N = 6$  spectral operator (where  $\alpha_j = \frac{1}{2} \cot\left(\frac{j\Delta x}{2}\right)$ )

$$\begin{pmatrix} u_x(x_1) \\ u_x(x_2) \\ u_x(x_3) \\ u_x(x_4) \\ u_x(x_5) \\ u_x(x_6) \end{pmatrix} = \begin{pmatrix} 0 & \alpha_1 & -\alpha_2 & \alpha_3 & -\alpha_4 & \alpha_5 \\ -\alpha_1 & 0 & \alpha_1 & -\alpha_2 & \alpha_3 & -\alpha_4 \\ \alpha_2 & -\alpha_1 & 0 & \alpha_1 & -\alpha_2 & \alpha_3 \\ -\alpha_3 & \alpha_2 & -\alpha_1 & 0 & \alpha_1 & -\alpha_2 \\ \alpha_4 & -\alpha_3 & \alpha_2 & -\alpha_1 & 0 & \alpha_1 \\ -\alpha_5 & \alpha_4 & -\alpha_3 & \alpha_2 & -\alpha_1 & 0 \end{pmatrix} \begin{pmatrix} u(x_1) \\ u(x_2) \\ u(x_3) \\ u(x_4) \\ u(x_5) \\ u(x_6) \end{pmatrix}$$

► full matrix  $\implies \sim \mathcal{O}(N^2)$  operations

# Obtaining the spectral differentiation matrix

- consider a **bounded & complete basis**:

$$u(x) = \sum_k a_k \phi_k(x) \implies u_x(x) = \sum_k a_k \frac{d\phi_k}{dx}(x)$$

- easy to compute, fast convergence, completeness  $\implies$  **Fourier series**:

$$u(x) = \sum_{k \in \mathbb{Z}} \hat{u}_k e^{ikx}$$

- for a periodic  $u \in C^\infty[0, 2\pi]$ , can show that:

$$\begin{aligned} \left\| u(x) - \sum_{k=1}^N \hat{u}_k e^{ikx} \right\|^2 &\leq \sum_{|k|>N} |\hat{u}_k|^2 \\ &\approx \left( \frac{2e^{-\alpha}}{1-e^{-\alpha}} \right) e^{-\alpha N} \end{aligned}$$

# Obtaining the spectral differentiation matrix

- discrete Fourier series:

$$u(x_j) = \frac{1}{2\pi} \sum_{k=-N/2+1}^{k=N/2} \hat{u}_k e^{ikx_j}$$

- discrete Fourier transform (DFT):

$$\hat{u}_k = \Delta x \sum_{j=1}^N u(x_j) e^{-ikx_j}, \forall k = -N/2+1, \dots, N/2$$

- "trigonometric polynomial" interpolant  $u(x) \approx \sum_{j=1}^N u(x_j) \frac{\sin\left(\frac{\pi x}{\Delta x}\right)}{\frac{2\pi}{\Delta x} \tan\left(\frac{\Delta x}{2}\right)}$   $\Rightarrow$

$$\begin{pmatrix} u_x(x_1) \\ \vdots \\ u_x(x_N) \end{pmatrix} = \begin{pmatrix} \ddots & & & & & \\ & \ddots & & & & \\ & & -\frac{1}{2} \cot\left(\frac{\Delta x}{2}\right) & 0 & \frac{1}{2} \cot\left(\frac{\Delta x}{2}\right) & -\frac{1}{2} \cot\left(\frac{2\Delta x}{2}\right) & \cdots \\ & & & \ddots & & & \\ & & & & \ddots & & \\ & & & & & \ddots & \end{pmatrix} \begin{pmatrix} u(x_1) \\ \vdots \\ u(x_N) \end{pmatrix}$$

# Computing the DFT

► **some notation:**  $f(x) : [0, 2\pi] \rightarrow \mathbb{R}$  with  $f(x_j) = j\Delta x$ ,  $\Delta x = 2\pi/N$ ,  $W_N = e^{-i\Delta x}$ ,

$$\begin{aligned} F(k) &= \sum_{j=0}^{N-1} f(x_j) e^{-ikj\Delta x} = \sum_{j=0}^{N-1} f(x_j) W_N^{kj} \\ f(x_j) &= \frac{1}{N} \sum_{k=0}^{N-1} F(k) e^{ikj\Delta x} = \sum_{j=0}^{N-1} f(x_j) W_N^{-kj} \end{aligned}$$

►  $N^2$  complex multiplications,  $N(N-1)$  complex additions  $\implies \mathcal{O}(N^2)$

► **note 1:** properties of complex exponential  $W_N = e^{-i\Delta x} \implies$

symmetry:  $W_N^k (N-j) = W_N^{-kj} = \overline{W_N^{kj}}$ ,   periodicity:  $W_N^{kj} = W_N^{k(j+N)} = W_N^{(k+N)j}$

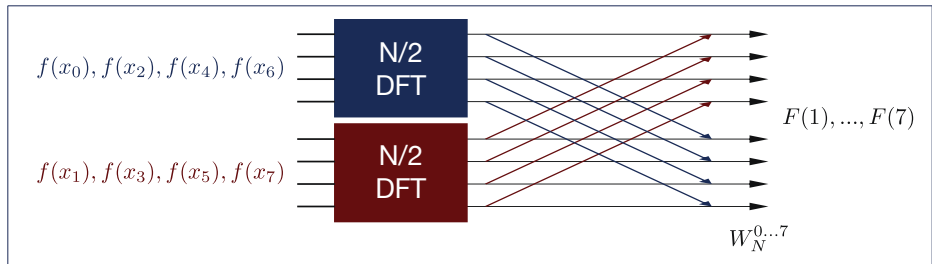
► **note 2:**  $2(N/2)^2 < N^2$  (two  $N/2$  DFTs faster than one  $N$  DFT)

$\implies$  calculate DFT recursively with smaller DFTs

# Fast fourier transforms

- ▶ 1965: James Cooley (IBM) & John Tukey (Princeton); 1805: Gauss (incidentally)
- ▶ decompose into even & odd:

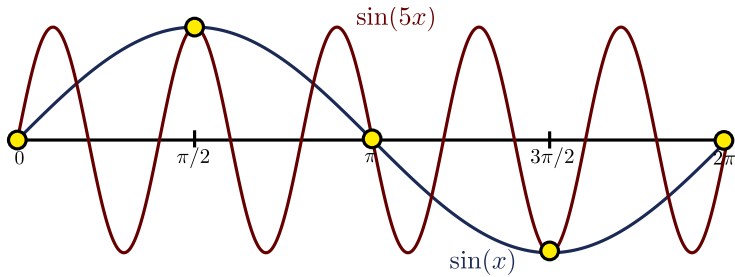
$$\begin{aligned} F(k) &= \sum_{n=0}^{N-1} f(x_j) W_N^{jk} = \sum_{j \text{ even}} + \sum_{j \text{ odd}} = \sum_{r=0}^{N/2-1} f(x_{2r}) W_{N/2}^{rk} + W_N^k \sum_{r=0}^{N/2-1} f(x_{2r+1}) W_{N/2}^{rk} \\ &= G(k) + W_N^k H(k) \end{aligned}$$



- ▶ repeat & work your way down ( $N/2 \rightarrow N/4 \rightarrow \dots$ )
- ▶ reduces complexity from  $\mathcal{O}(N^2)$  to  $\mathcal{O}(N \log N)$

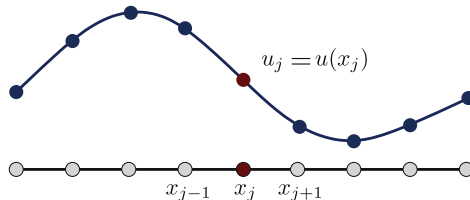
# Grid aliasing & Nyquist sampling theorem

- highest wavenumber resolved:  $|k| = N/2$



# A quick example

► Burgers' equation:  $u_t + (1+u)u_x = \mu u_{xx}$



► approximate spatial derivatives:

Finite differences

$$u_x(x_j) \approx \frac{u(x_{j+1}) - u(x_{j-1})}{2\Delta x}$$

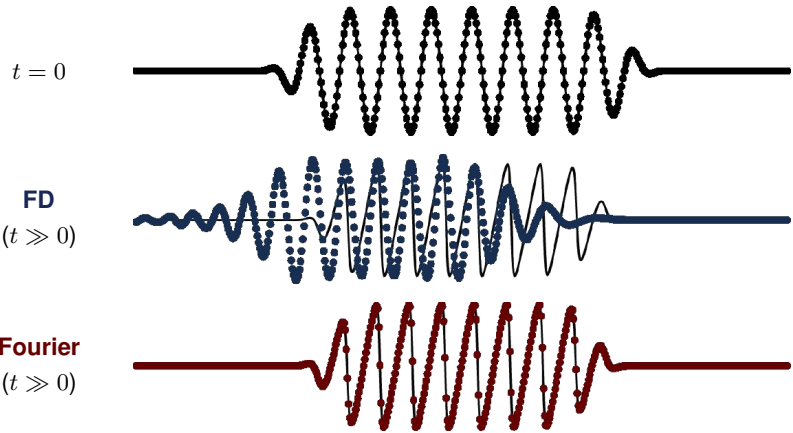
(Truncated) Fourier series

$$u_x(x_j) \approx \sum_{k=-N/2}^{k=N/2} i k a_k e^{ikx_j}$$

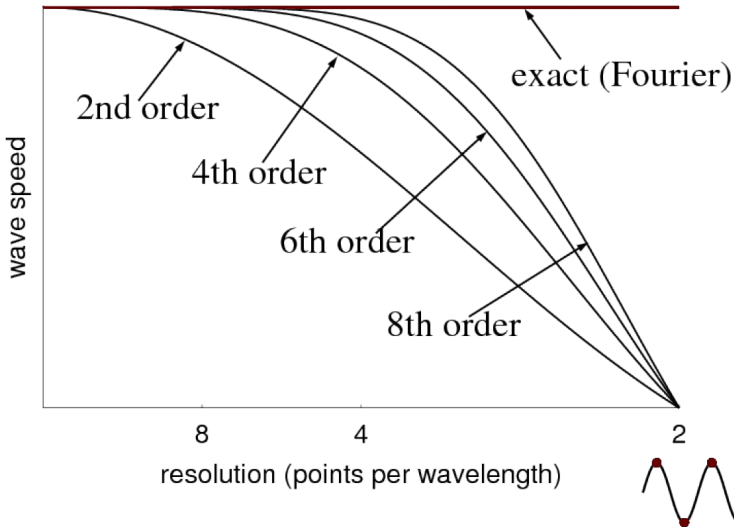
► evolve in time (Euler, Runge-Kutta, etc.)

# A quick example

- numerical **dispersion errors** ("pollution")



# Approximating wave speeds

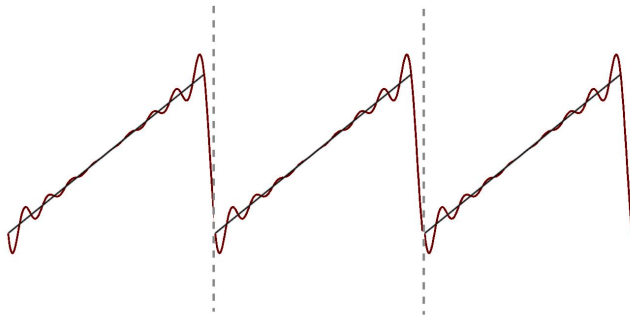


# A major bottleneck of finite Fourier sums

- ▶ periodic assumptions:



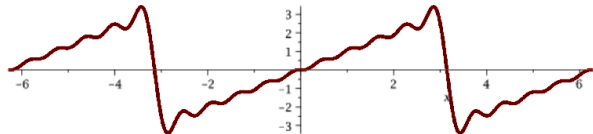
- ▶ assumed jump  $\implies$  **Gibbs phenomenon:**



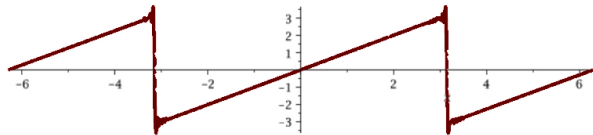
# Gibbs phenomenon

►  $f(x) = x, x \in [-\pi, \pi] \implies f(x) \approx 2 \left( \sin(x) - \frac{1}{2} \sin(2x) + \frac{1}{3} \sin(3x) - \frac{1}{4} \sin(4x) + \dots \right)$

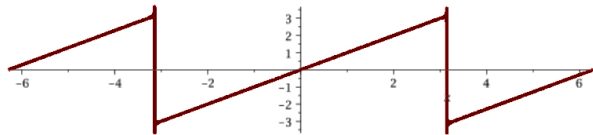
10 terms



100 terms



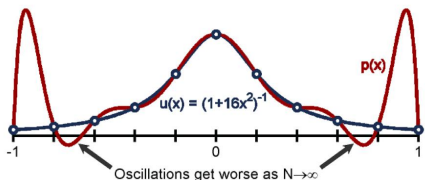
1000 terms



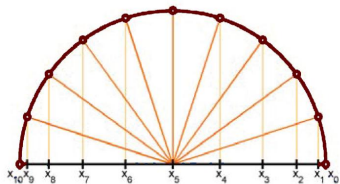
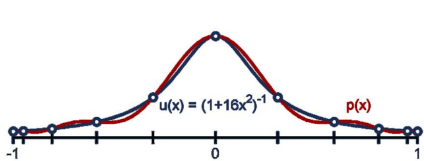
# Chebyshev polynomials

- algebraic polynomial interpolation  $p_N(x) = a_0 + a_1x + \dots + a_Nx^N$ :

Runge phenomenon on equidistant grids



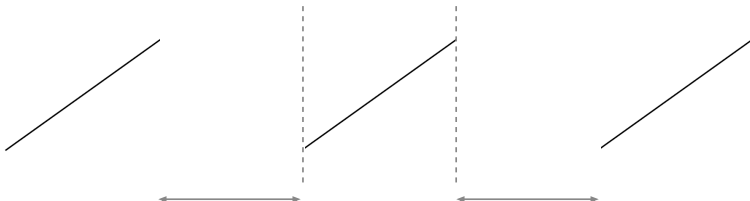
- Chebyshev points  $x_j = \cos\left(\pi \frac{j}{N}\right)$ :



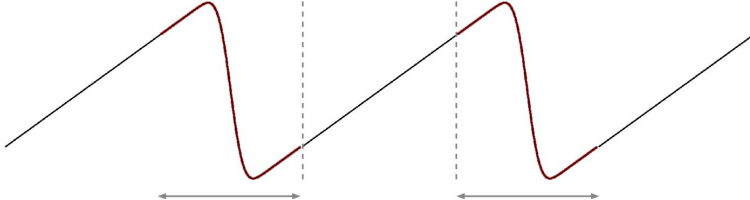
- works well **except for dynamics** ( $\Delta t \propto \Delta x^2$  or higher)

# Fourier continuation (FC) for non-periodic functions

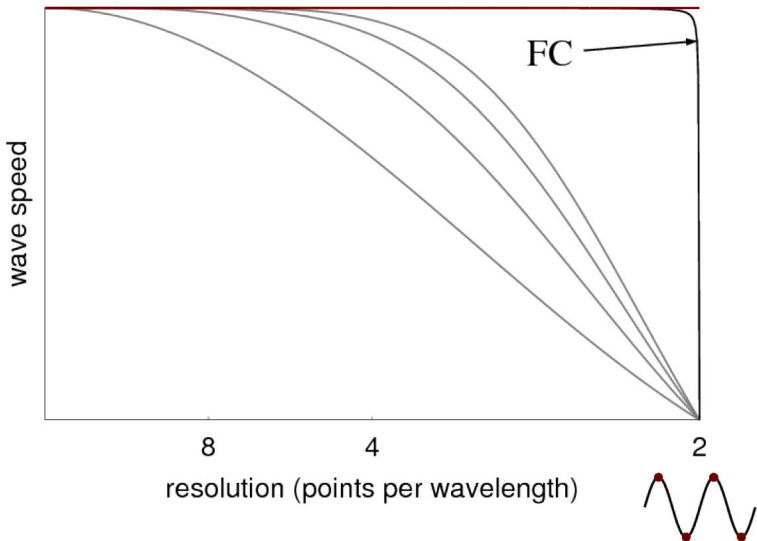
- ▶ **translate function** (leave a gap outside physical domain):



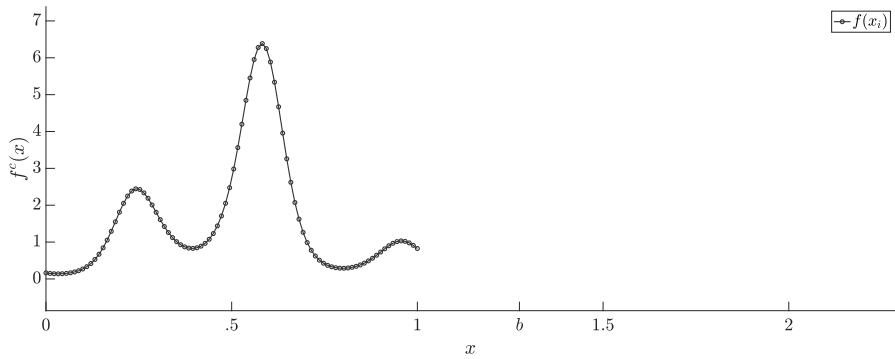
- ▶ **fill with smooth transition:**



## FC maintains nice dispersion properties



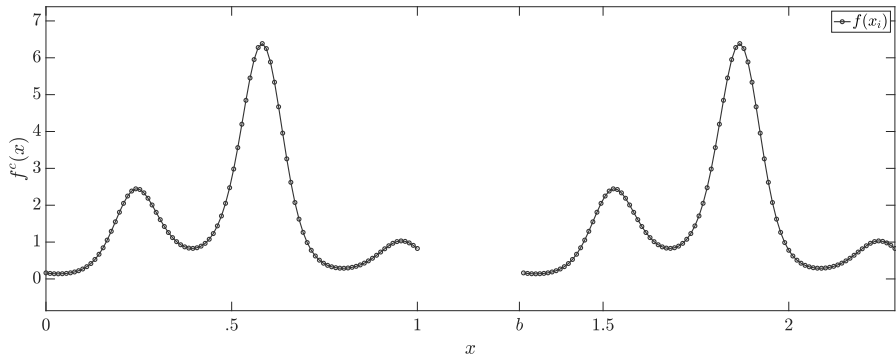
# Principles of FC



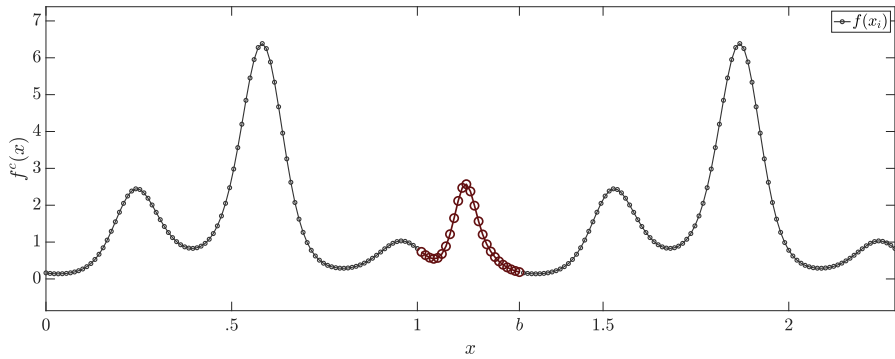
- ▶ given point values of the (non-periodic) function  $f : [0, 1] \rightarrow \mathbb{R}$ :

$$f(x_i), \quad x_i = i\Delta x, \quad i = 0, \dots, N-1, \quad \Delta x = 1/(N-1)$$

# Principles of FC



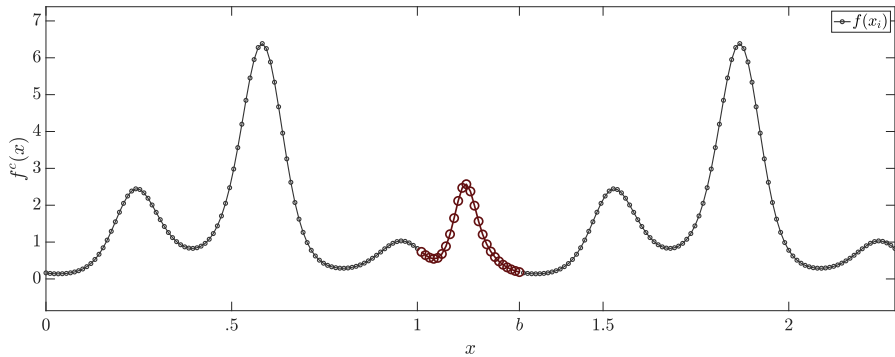
# Principles of FC



► construct a  $b$ -periodic Fourier series ( $b > 1$ ):

$$f^c(x) = \sum_{k=-M}^M a_k e^{\frac{2\pi i k x}{b}}, \quad f^c(x_i) = f(x_j), i = 0, \dots, N-1$$

# Principles of FC

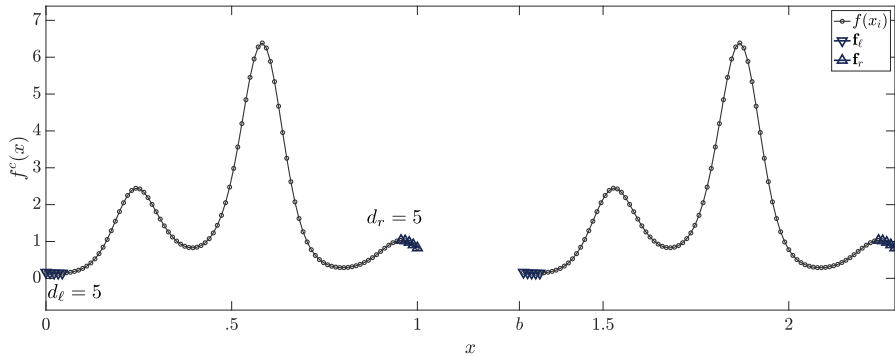


► find coefficients of  $f^c(x) = \sum_{k=-M}^M a_k e^{\frac{2\pi i k x}{b}}$ :

$$\min_{\mathbf{a}=(a_{-M}, \dots, a_M)^T} \|B\mathbf{a} - (f(x_0), \dots, f(x_{N-1})^T)\|_2, \quad B_{mn} = \begin{cases} e^{\frac{2\pi i m x_n}{b}} & m \leq M \\ e^{\frac{2\pi i (M-m) x_n}{b}} & \text{otherwise} \end{cases}$$

► solve by, e.g., a truncated SVD  $\implies \mathcal{O}(N^3)$  cost per continuation

# Accelerated FC



► choose small numbers of  $d = d_\ell, d_r$  “matching points”:

$$\mathbf{f}_\ell = (f(x_0), \dots, f(x_{d_\ell-1}))^T, \quad \mathbf{f}_r = (f(x_{N-d_r}), \dots, f(x_{N-1}))^T$$

# Accelerated FC

- **precompute** a “continuation basis” of  $C$  points:

1) construct a **projection** of  $\mathbf{f}_\ell$  ( $\mathbf{f}_r$ ) onto a Gram polynomial **interpolating basis**:

- orthonormalize Vandermonde matrix (WLOG,  $d = d_\ell, d_r$ ):

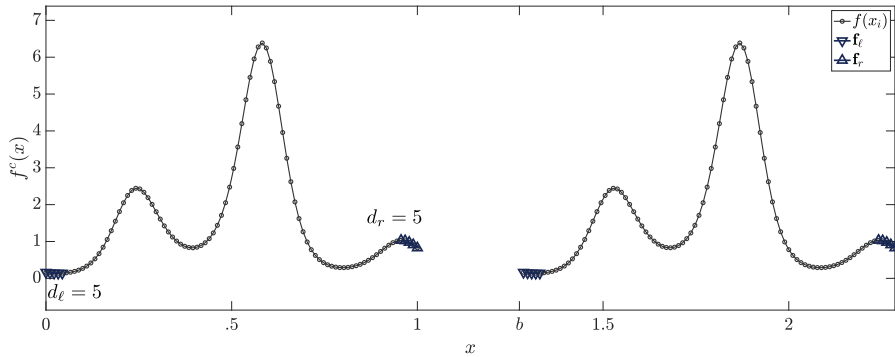
$$P = \begin{pmatrix} 1 & x_0 & (x_0)^2 & \dots & (x_0)^{d-1} \\ 1 & x_1 & (x_1)^2 & \dots & (x_1)^{d-1} \\ \vdots & \vdots & \vdots & \vdots & \vdots \\ 1 & x_{d-1} & (x_{d-1})^2 & \dots & (x_{d-1})^{d-1} \end{pmatrix} = QR$$

2) **construct extensions** of each Gram poly  $q_j$  (columns of  $Q$ ):

- find coefficients of the band-limited trig polynomial ( $M = (d+C)/2$ ):

$$q_j(x) = \sum_{k=-M}^M a_k e^{\frac{2\pi i k x}{(d+C-1)h}} \rightarrow \min_{\mathbf{a}=(a_{-M}, \dots, a_M)^T} \left\| B\mathbf{a} - \begin{pmatrix} q_j \\ \mathbf{0} \end{pmatrix} \right\|_2$$

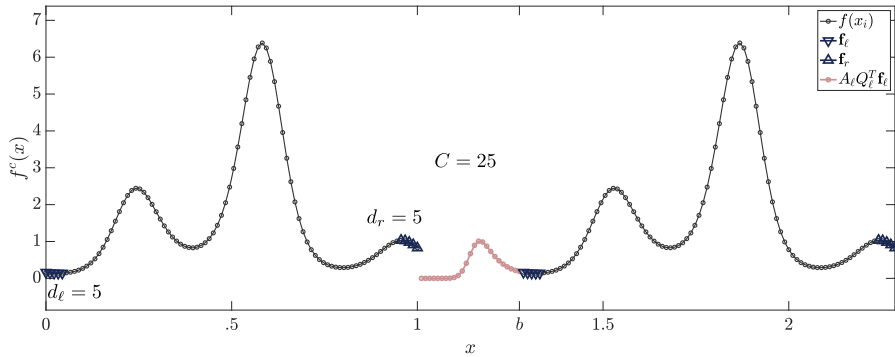
# Accelerated FC



- ▶ choose small numbers of  $d = d_\ell, d_r$  “matching points”:

$$\mathbf{f}_\ell = (f(x_0), \dots, f(x_{d_\ell-1}))^T, \quad \mathbf{f}_r = (f(x_{N-d_r}), \dots, f(x_{N-1}))^T$$

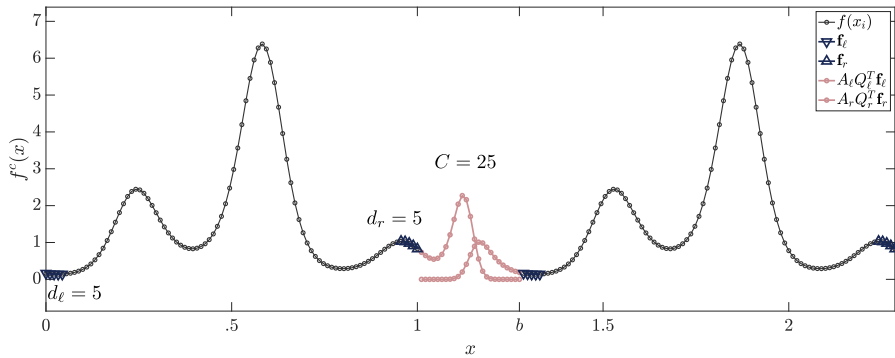
# Accelerated FC



- ▶ project left points  $d = d_\ell$  onto precomputed continuation basis:

$$A_\ell Q_\ell^T \mathbf{f}_\ell$$

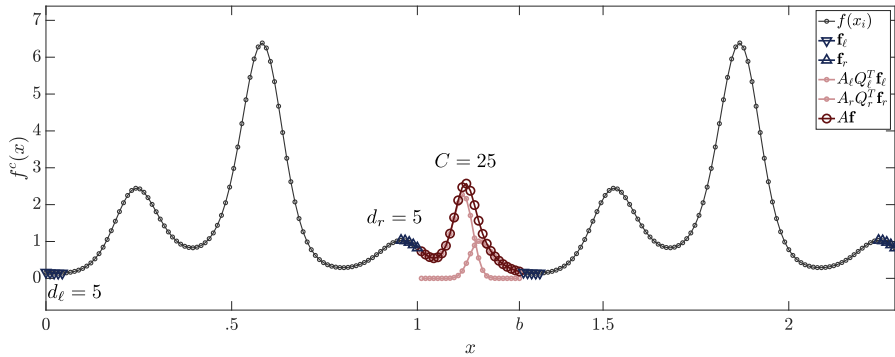
# Accelerated FC



- ▶ project right points  $d = d_r$  onto precomputed continuation basis:

$$A_r Q_r^T \mathbf{f}_r$$

# Accelerated FC



► form the full continuation via sum:

$$A\mathbf{f} = A_\ell Q_\ell^T \mathbf{f}_\ell + A_r Q_r^T \mathbf{f}_r$$

(auxiliary polynomial of periodicity  $[1 - \delta_r, 2b - (1 - \delta_\ell)]$  where  $\delta_{\ell,r} = d_{\ell,r} \Delta x$  )

# A modified operator for Neumann-like boundaries

- if **derivative values** at boundary, orthonormalize instead:

$$P_{\ell,\text{mod}} = \begin{pmatrix} 1 & x_0 & (x_0)^2 & \dots & (x_0)^{d_\ell-1} \\ 1 & x_1 & (x_1)^2 & \dots & (x_1)^{d_\ell-1} \\ \vdots & \vdots & \vdots & \vdots & \vdots \\ 0 & 1 & 2x_{d_\ell-1} & \dots & (d_\ell-1)(x_{d_\ell-1})^{d_\ell-2} \end{pmatrix} = Q_{\ell,\text{mod}} R_{\ell,\text{mod}}$$

- construct a **new projection**  $\hat{Q}_\ell = (Q_\ell R_\ell R_{\ell,\text{mod}}^{-1} Q_{\ell,\text{mod}}^T)^T$  s.t.:

$$A\mathbf{f} = A_\ell \hat{Q}_\ell^T \hat{\mathbf{f}}_\ell + A_r Q_r^T \mathbf{f}_r, \quad \hat{\mathbf{f}}_\ell = (f(x_0), \dots, f(x_{d_\ell-2}), f_x(x_{d_\ell-1}))^T$$

- useful for, e.g., **elastic traction, convective flux, ODE-PDE coupling**

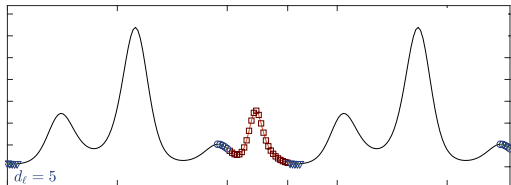
 [Amlani, et al., under review/arXiv:2112.05257 \(2023\)](#)

 [Amlani & Pahlevan, Journal of Computational Physics \(2020\)](#)

 [Amlani & Bruno, Journal of Computational Physics \(2016\)](#)

# Building PDE solvers with the FC approach

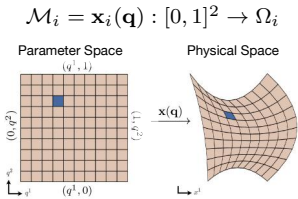
High-order Fourier series of non-periodic functions



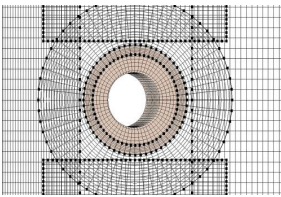
Highly-accurate derivatives via FFT

$$\begin{aligned}f^c &\leftarrow f \\f^c &= \sum_{-M}^M a_k e^{\frac{2\pi i k x}{b}} \\ \frac{df^c}{dx} &= \sum_{-M}^M \frac{2\pi i k}{b} a_k e^{\frac{2\pi i k x}{b}}\end{aligned}$$

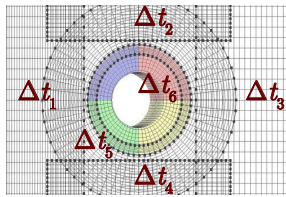
Curvilinear coordinate systems



Overset domains



Efficient parallelization (HPC)



[Amlani, et al., under review/arXiv:2112.05257 \(2023\)](#)

[Amlani, et al., Geophysical Journal International \(2022\)](#)

[Amlani & Pahlevan, Journal of Computational Physics \(2020\)](#)

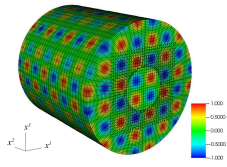
[Amlani & Bruno, Journal of Computational Physics \(2016\)](#)

# High-order convergence

► maximum errors over all space and time for increasing spatial discretization

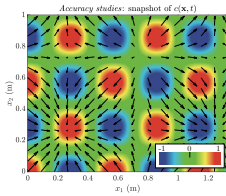
## Elastodynamics (hyperbolic)

(through 10 000 timesteps, up to 480 cores)



## Advection-diffusion (hyperbolic+parabolic)

(through 5 000 timesteps)



$N$	$L_{\text{err}}^{\infty}$	$\mathcal{O}(L^{\infty})$
792 000	$8.29 \times 10^{-5}$	—
2 673 000	$9.37 \times 10^{-6}$	<b>5.38</b>
6 336 000	$2.00 \times 10^{-6}$	<b>5.37</b>
12 375 000	$6.51 \times 10^{-7}$	<b>5.03</b>

$N$	$L_{\text{err}}^{\infty}$	$\mathcal{O}(L^{\infty})$
30	$7.03 \times 10^{-3}$	—
60	$2.11 \times 10^{-4}$	<b>5.18</b>
120	$6.52 \times 10^{-6}$	<b>5.08</b>
240	$2.07 \times 10^{-7}$	<b>5.00</b>

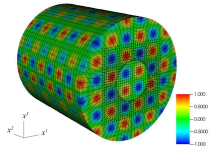
[Amlani, et al., under review/arXiv:2112.05257 \(2023\)](#)

[Amlani & Bruno, Journal of Computational Physics \(2016\)](#)

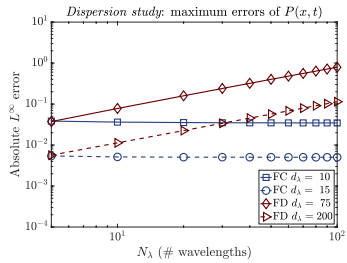
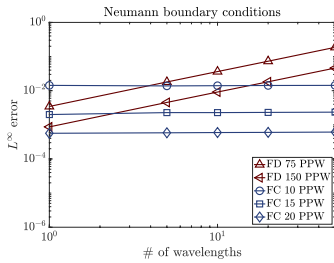
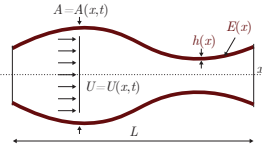
# No dispersion errors

► maximum errors over all space and time (one period) for increasing domain size

Elastodynamics (hyperbolic)



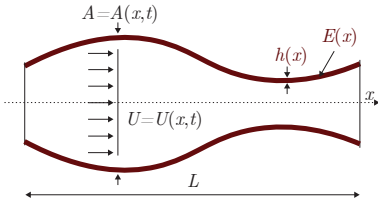
Nonlinear hemodynamics (hyperbolic+parabolic)



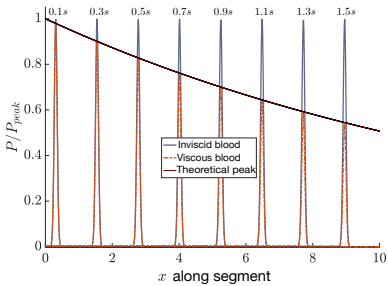
Amlani & Pahlevan, Journal of Computational Physics (2020)

Amlani & Bruno, Journal of Computational Physics (2016)

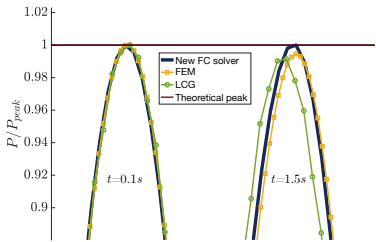
# Comparisons with other solvers: hemodynamics equations



FC single pulse pressure benchmark



FC solver comparison (inviscid blood)



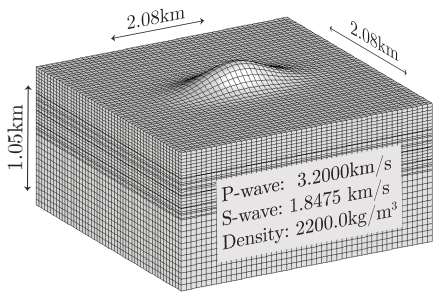
Amlani & Pahlevan, to be submitted (2023)

# Comparisons with other solvers: elastodynamics equations

(a classical problem inspired by the 1994 Northridge, California earthquake)

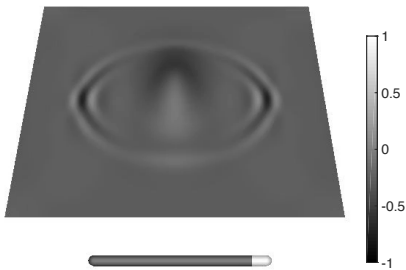
► **vertically-incident shear wave** polarized along minor axis (180m-tall hill)

3D linear elastodynamics model (explicit FC)



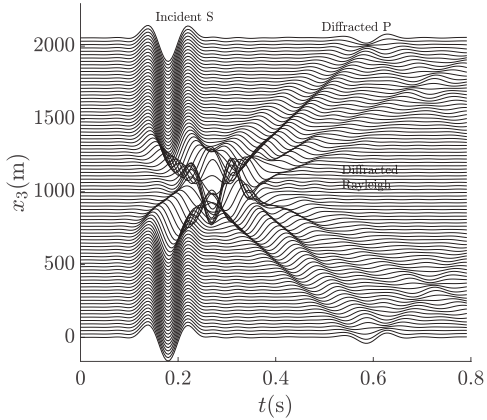
Earth material params (traction-free surface)

Normalized in-plane displacement



# Comparisons with other solvers: elastodynamics equations

In-plane  $u_3$  along  $x_3$ -axis



► 3D spectral element method

(Komatitsch & Vilotte, 1999):

$$\underline{N = 4,935,953}$$

► 3D finite difference method

(Appelö & Petersson, 2009):

$$\underline{N = 109,808,412}$$

► 3D FC method

(Amlani & Bruno, 2016):

$$\underline{N = 143,871}$$

(58 seconds on 96 cores)



Amlani & Bruno, *Journal of Computational Physics* (2016)

# Using FC-based PDE solvers for scientific & engineering problems

*predictions & insights into the underlying physics*

## Applications to the non-destructive testing of materials

Primary collaborators:

J. Carlos López-Vázquez (*applied physics/optics*,  Universidade de Vigo)

Oscar P. Bruno (*applied/computational mathematics*,  Caltech)

# Motivation

Pipelines



Aircraft



Railroads 2



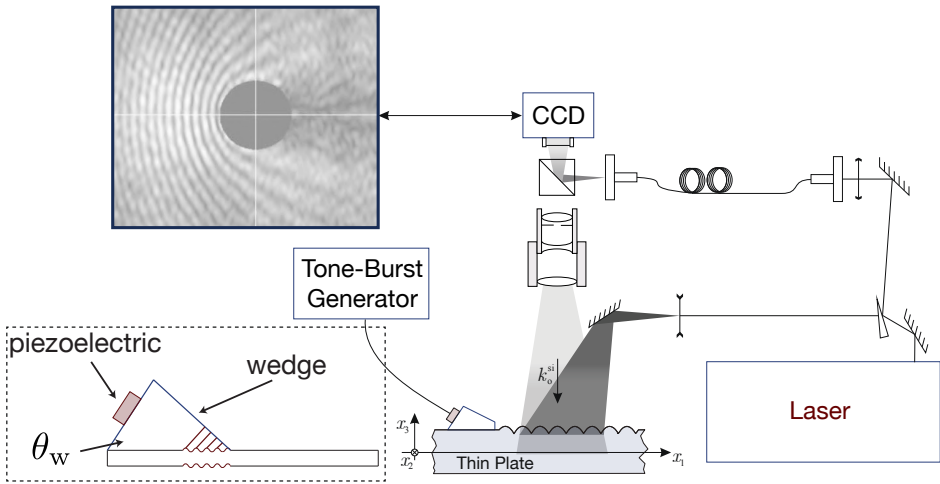
Bridges



# Ultrasonic NDT for thin plate-like structures

- ▶ laboratory measurements via **pulsed television holography** (PTVH)

(group of J. Carlos López-Vázquez, Universidade de Vigo, Spain)

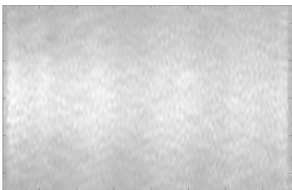


# Measured displacement maps (steady-state example)

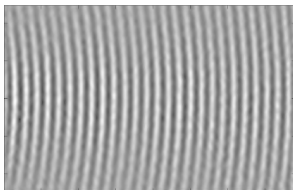
- ▶ 300mm × 100mm **aluminum plates** of thickness  $h = 10\text{mm}$

Incident (reference) fields

(complex modulus/amplitude)

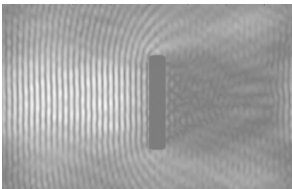


(real amplitude)

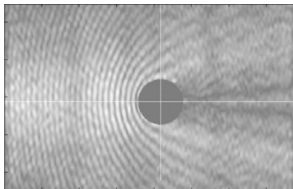


Scattering by thru-holes (complex modulus)

(4.4mm × 24mm)



(12mm diameter)



## Quick review of classical plate (guided wave) theory

- ▶ assume **displacement**  $\mathbf{u} = \mathbf{u}(\mathbf{x}, t)$  in a homogeneous linear elastic solid  $\Omega$ :  
 $(\lambda, \mu$ : Lamé material parameters;  $\rho$ : density)

$$\rho \ddot{\mathbf{u}} = \mu \nabla^2 \mathbf{u} + (\lambda + \mu) \nabla \nabla \cdot \mathbf{u} + \mathbf{f}, \quad \mathbf{x} \in \Omega \subset \mathbb{R}^3, t \in \mathbb{R}$$

- ▶ **Helmholtz decomposition** (scalar & vector potentials), absence of body forces:

$$\mathbf{u}(\mathbf{x}, t) = \nabla \phi(\mathbf{x}, t) + \nabla \times \psi(\mathbf{x}, t)$$

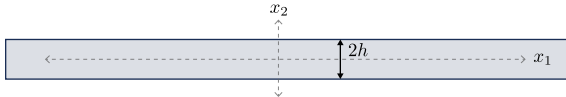
⇒

$$\nabla[(\lambda + 2\mu) \nabla^2 \phi - \rho \phi_{tt}] + \nabla \times [\mu \nabla^2 \psi - \rho \psi_{tt}] = 0$$

- ▶ scalar (*longitudinal*) & vector (*transverse or shear*) wave equations:

$$\begin{cases} \phi_{tt} &= c_L^2 \nabla^2 \phi \\ c_L &= \sqrt{\frac{\lambda + 2\mu}{\rho}} \end{cases} \quad \& \quad \begin{cases} \psi_{tt} &= c_T^2 \nabla^2 \psi \\ c_T &= \sqrt{\frac{\mu}{\rho}} \end{cases} \quad \left( \nu = \frac{\lambda}{2(\lambda + \mu)} \right)$$

# Quick review of classical plate theory



► for **general solutions**  $\phi = \Phi(x_2) \exp(ikx_1 - \omega t)$ ,  $\psi = \Psi(x_2) \exp(ikx_1 - \omega t)$  :

(symmetric)

$$u_1 = i(B\xi \cos(\alpha x_2) + C\beta \cos(\beta x_2))e^{i(x_1 - \omega t)}$$

$$u_2 = (-B\alpha \sin(\alpha x_2) + C\xi \sin(\beta x_2))e^{i(x_1 - \omega t)}$$

$$\left( \alpha^2 = \omega^2/c_L^2 - k^2, \quad \beta^2 = \omega^2/c_T^2 - k^2 \right)$$

(antisymmetric)

$$u_1 = i(\xi A \sin(\alpha x_2) - D\beta \sin(\beta x_2))e^{i(x_1 - \omega t)}$$

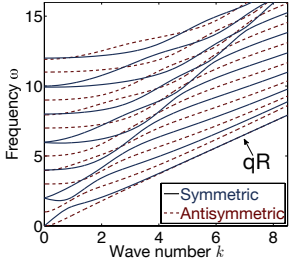
$$u_2 = (A\alpha \cos(\alpha x_2) + D\xi \cos(\beta x_2))e^{i(x_1 - \omega t)}$$

► for **traction-free** ( $\sigma \cdot \mathbf{n} = 0$ ) boundaries:

$$\frac{\tan(\beta h)}{\tan(\alpha h)} = - \left( \frac{4\alpha\beta k^2}{(k^2 - \beta^2)^2} \right)^{\pm 1}$$

$$\begin{cases} +1 & \text{symmetric} \\ -1 & \text{antisymmetric} \end{cases}$$

“quasi-Rayleigh” waves



# Modeling experiments w/Helmholtz equations (scalar acoustics)

- ▶ “membrane-like” waves over the guiding plane (*Achenbach 2003*):

$$u_1(x_1, x_2, x_3, t) = \frac{1}{k} V(x_2) e^{i\omega t} \frac{\partial}{\partial x_1} \phi(x_1, x_3),$$

$$u_2(x_1, x_2, x_3, t) = W(x_2) e^{i\omega t} \phi(x_1, x_3), \quad \iff \quad \nabla^2 \phi + k^2 \phi = 0$$

$$u_3(x_1, x_2, x_3, t) = \frac{1}{k} V(x_2) e^{i\omega t} \frac{\partial}{\partial x_3} \phi(x_1, x_3),$$

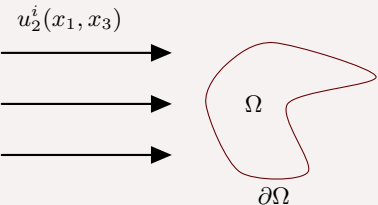
- ▶ for a given mode, at  $x_2 = C = \text{const}$  (**observable plate surface**):

$$\nabla^2 u_2 + k^2 u_2 = 0, \quad u_2 = u_2^i + u_2^s$$

▶  $\mathbf{x} = (x_1, x_3) \notin \Omega :=$  exterior scattering problem

▶  $u_2(\mathbf{x}) :=$  out-of-plane displacement

▶  $\left. \frac{\partial u_2}{\partial n} \right|_{\Gamma} = g :=$  Neumann BCs on  $\partial\Omega$



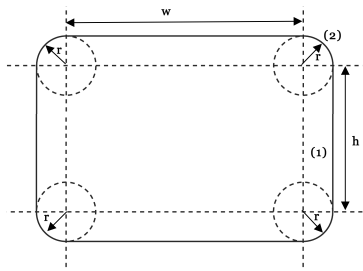
# High-order first kind integral equation (IE) solvers

- ▶ using trigonometric interpolation

Boundary integral formulation ( $\mathbf{r} \in \Omega$ )

$$u_2(\mathbf{r}) = \int_{\Gamma} \frac{\partial G_k(\mathbf{r}, \mathbf{r}')}{\partial \mathbf{n}'_{\mathbf{r}'}} \mu(\mathbf{r}') d\ell'$$

$C^\infty$  smoothed piecewise maps (POU)



- ▶ define the **hypersingular operator**:

$$N(\mu)(\mathbf{r}) = \lim_{z \rightarrow 0} \frac{\partial}{\partial \mathbf{n}_{\mathbf{r}}} \int_{\Gamma} \frac{\partial G_k(\mathbf{r}, \mathbf{r}' + \mathbf{n}_{\mathbf{r}'})}{\partial \mathbf{n}'_{\mathbf{r}'}} \mu(\mathbf{r}') d\ell'$$

- ▶  $\mu$  is the (unique) solution of the **first-kind IE**:

$$N(\mu) = g$$

e.g.,  $x_{12}(s) = x_1(s)P(s) + x_2(s)(1 - P(s))$

- ▶ reformulate in terms of tangential derivatives

- ▶ trig interp of  $\mu_j$  + exact diff/int of trig monomials

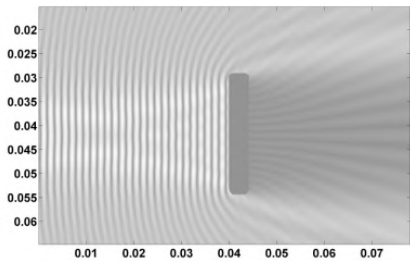
$$P(s) = \begin{cases} 0, & s \leq s_1 \\ 1 - e^{\left(\frac{2e^{-1/\tau}}{\tau-1}\right)}, & s_1 < s, \tau = \frac{s-s_1}{1-s_1} \end{cases}$$

 López-Vázquez, Amlani, et al., *Optical Engineering* (2010)

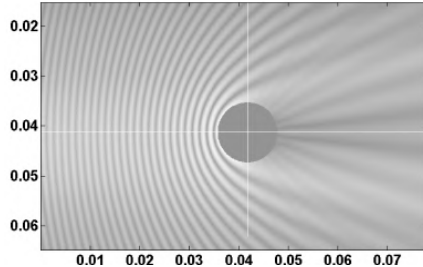
# High-order convergence

► maximum errors over all space for increasing boundary discretization

“Slot-shaped” defect



Circular defect



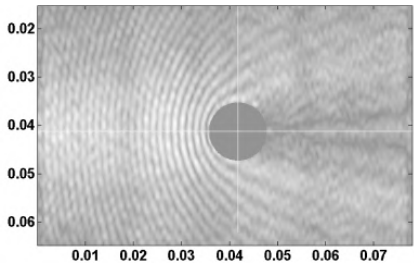
$N$	iterations	surface density $L_{\text{err}}^{\infty}$	$\mathcal{O}(L^{\infty})$	farfield $L_{\text{err}}^{\infty}$	$\mathcal{O}(L^{\infty})$
256	31	3.17e-1	—	3.92e-1	—
512	28	1.50e-4	<b>11.04</b>	1.76e-5	<b>14.44</b>
1024	34	3.95e-7	<b>8.56</b>	3.77e-9	<b>12.19</b>

López-Vázquez, Amlani, et al., *Optical Engineering* (2010)

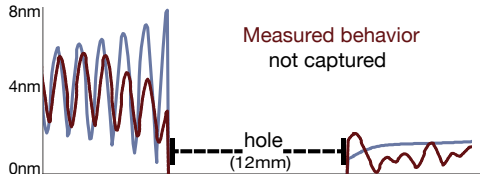
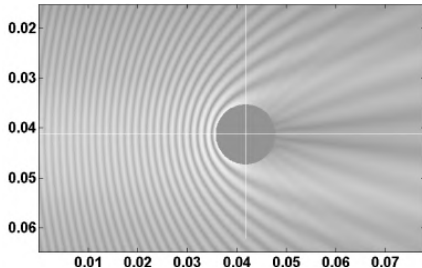
# Experiment vs simulation

► **out-of-plane** displacement (complex amplitude)

Experiment



Simulation

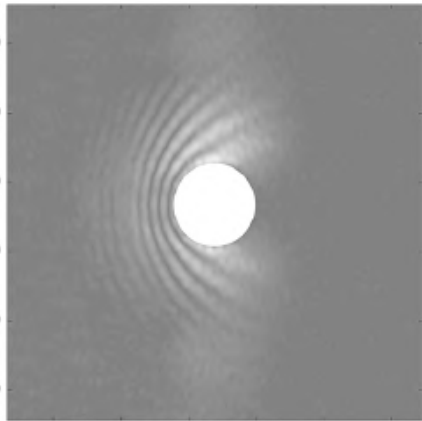


López-Vázquez, Amlani, et al., *Optical Engineering* (2010)

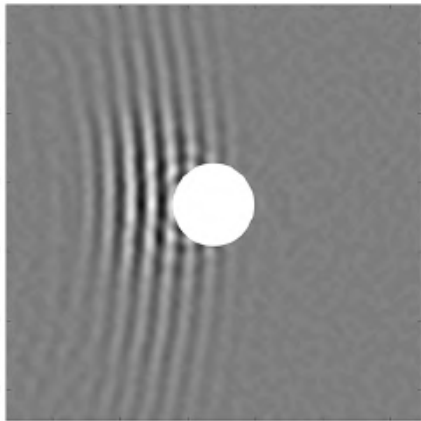
# Returning to 3D dynamical equations

► high-frequency elastic wave propagation

Experiment (complex amplitude)



Experiment (real amplitude)



# Modeling experiments w/Cauchy-Navier equations (elastodynamics)

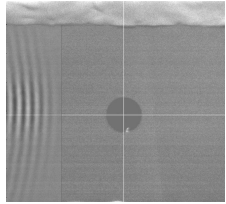
- the first FC solver for **variable coefficient 3D equations & Neumann boundaries**

$$\rho(\mathbf{x})\mathbf{u}_{tt}(\mathbf{x}, t) = \nabla \cdot [\mu(\mathbf{x})(\nabla \mathbf{u}(\mathbf{x}, t) + \nabla \mathbf{u}^T(\mathbf{x}, t)) + \lambda(\mathbf{x})(\nabla \cdot \mathbf{u}(\mathbf{x}, t))I] + \mathbf{f}(\mathbf{x}, t)$$

- $\mathbf{u}(\mathbf{x}, t)$  := 3D displacement at  $\mathbf{x} \in \Omega$ , time  $t$
- $\lambda(\mathbf{x}), \mu(\mathbf{x}), \rho(\mathbf{x})$  := material parameters (spatially-varying)
- $\sigma \cdot \mathbf{n} = \mathbf{T}(\mathbf{x}, t), \sigma_{ij} = c_{ijk\ell} \frac{\partial u^k}{\partial x^\ell}$  := traction boundary conditions on  $\partial\Omega$

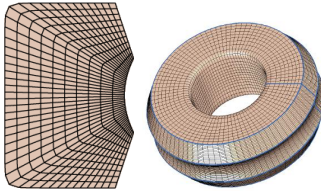
Physical domain

(material sample)



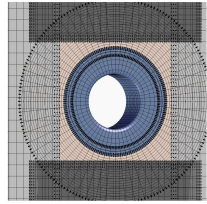
Curvilinear mappings

(e.g., superellipse + transfinite interp.)



Computational domain

(overset decomposition)

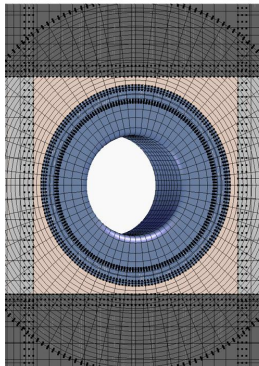


Amlani & Bruno, *Journal of Computational Physics* (2016)

# Parallel scalability

► CPU seconds per million unknowns per timestep :=

$$S = \frac{(\# \text{ cores}) \times (\text{total time})}{3 \times (\# \text{ grid pts}) / 10^6}$$



A weak test for 3D elastodynamics (six curvilinear volumes)

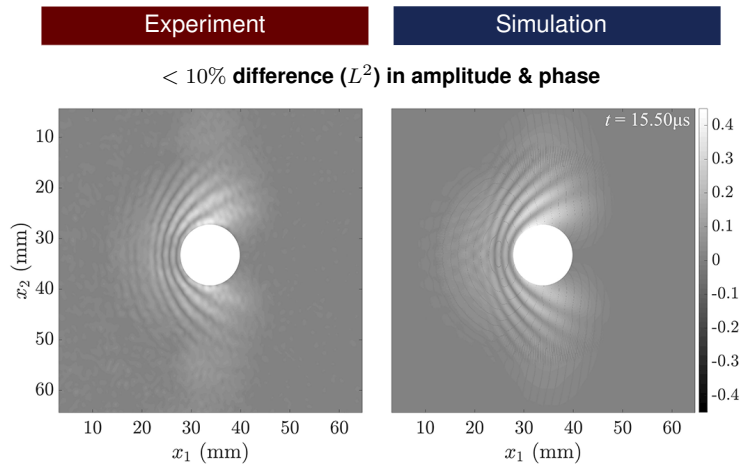
# grid pts	# cores	$L_{\text{err}}^\infty$	$\mathcal{O}(L^\infty)$	$S$
377 460	120	$1.70 \times 10^{-1}$	—	1.61 sec
3 033 360	360	$7.98 \times 10^{-3}$	<b>4.41</b>	1.54 sec
10 252 980	480	$1.04 \times 10^{-3}$	<b>5.03</b>	1.65 sec

A strong test for 3D elastodynamics (six curvilinear volumes)

# grid pts	# cores	$L_{\text{err}}^\infty$	$O(L^\infty)$	$S$
3 033 360	240	$7.89 \times 10^{-3}$	—	<b>1.51 sec</b>
—	360	$7.98 \times 10^{-3}$	—	<b>1.55 sec</b>
—	480	$8.32 \times 10^{-3}$	—	<b>1.45 sec</b>

# Experiment vs simulation

► normalized **complex amplitude** (out-of-plane displacement), 512 processing cores

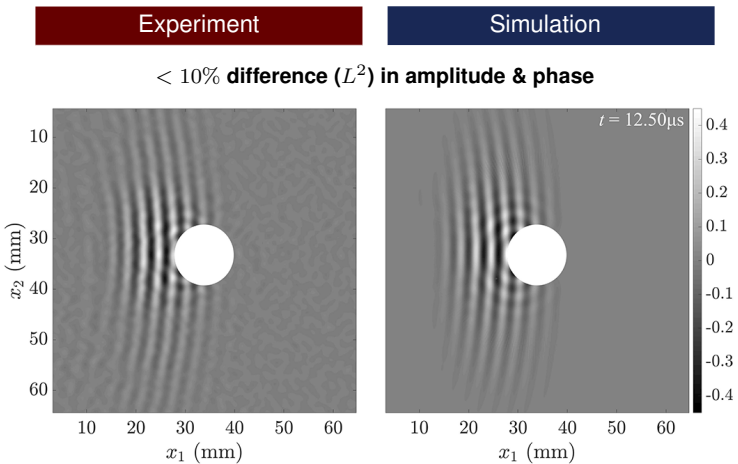


[Amlani, et al., arXiv:1905.05289 \(2019\)](#)

[Amlani & Bruno, Journal of Computational Physics \(2016\)](#)

# Experiment vs simulation

- normalized **real amplitude** (out-of-plane displacement), 512 processing cores



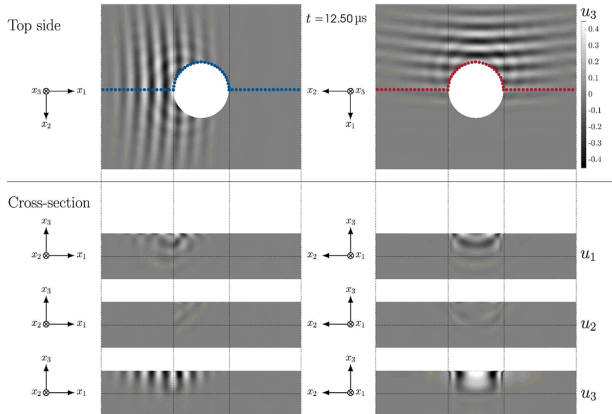
 [Amlani, et al., arXiv:1905.05289 \(2019\)](#)

 [Amlani & Bruno, Journal of Computational Physics \(2016\)](#)

# Observing a mode conversion in 3D simulations

► a first look inside the hole: all three displacement components simulated

Simulation (two views, real amplitudes)



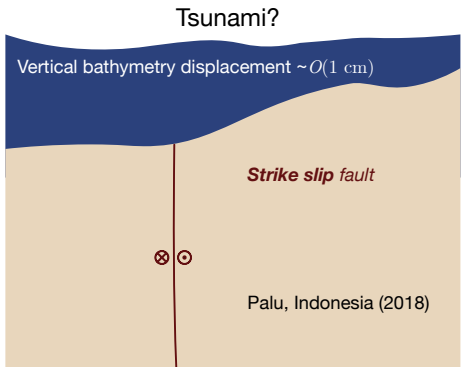
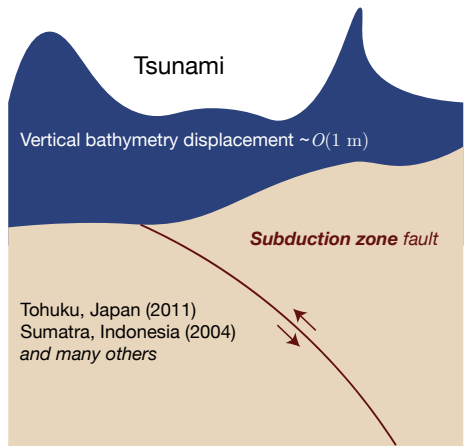
## Applications to studying seismogenic tsunamis

Primary collaborator:

Harsha S. Bhat (seismology/earth sciences,  CNRS/École Normale Supérieure Paris)

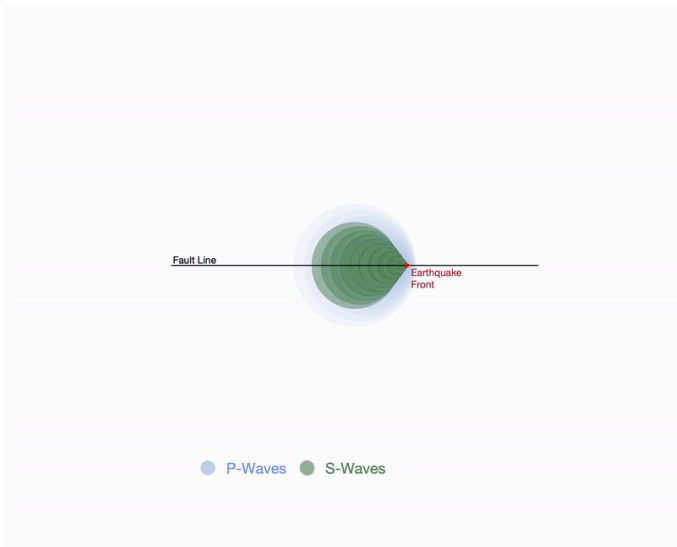
# Motivation

- ▶ the mystery of the 2018 Palu, Indonesia tsunami

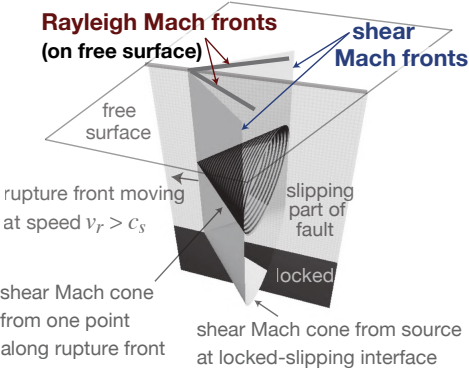


# What is a supershear rupture?

- ▶ ground rupture travels at speeds in **excess of the shear wave velocity**

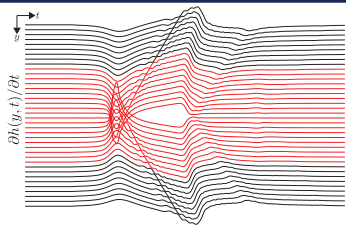


# Modeling & theory via simulation

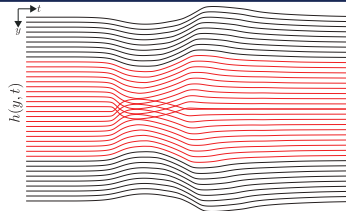


(Dunham & Bhat, 2008)

Vertical velocity



Vertical displacement

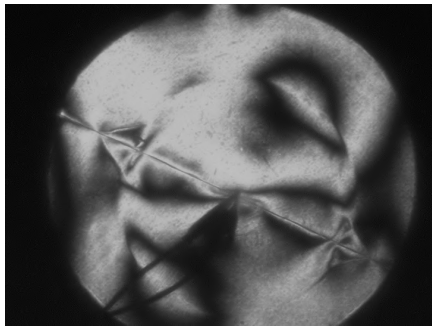


# Modeling & theory via experiment

- ▶ trailing Rayleigh wave
- ▶ fault parallel velocity > fault normal
- ▶ dilatational field

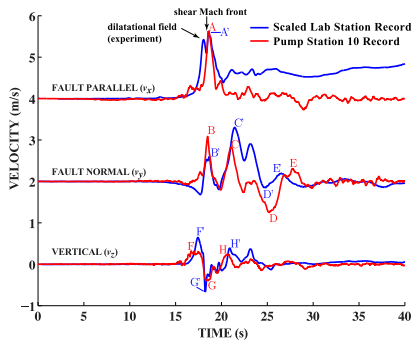
## Laboratory evidence

(Mello, et al., 2010, 2016)



## 2002 Denali experiments

(Mello, et al., 2014)



# First near field evidence of a supershear rupture at Palu

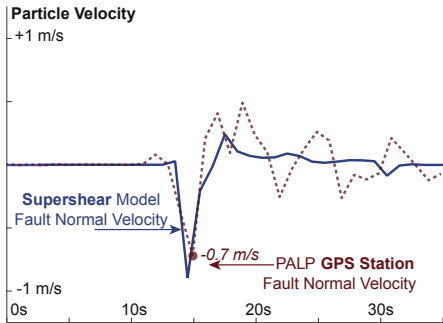
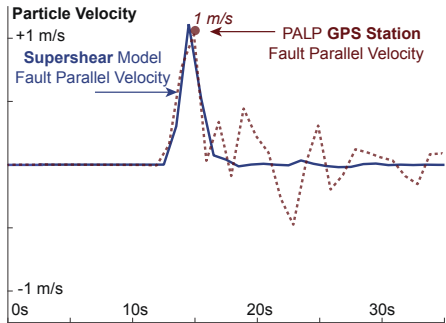
► trailing Rayleigh wave

► fault parallel velocity > fault normal

► dilatational field

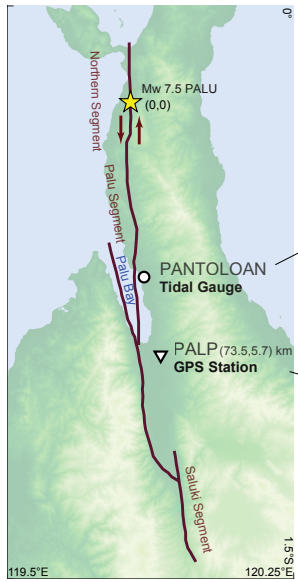
Parallel: GPS (PALP, 1Hz) & rupture model

Normal: GPS (PALP, 1Hz) & rupture model

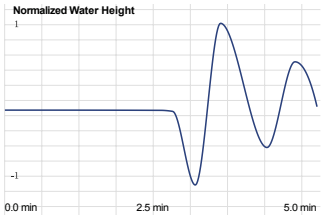


Amlani, et al., *Geophysical Journal International* (2022)

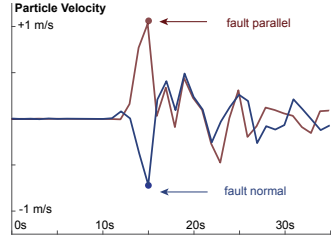
# Measured data during the 2018 Palu events



## PANT CCTV Camera Records

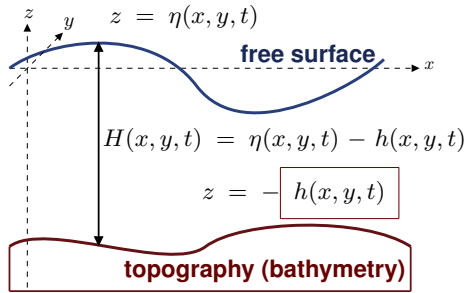


## PALP GPS Station



# Modeling with dynamic ground motion

► nonlinear shallow water wave equations w/**time-dependent displacement & velocity**



$\mathbf{u}$  := velocity

$H$  := total height

$\eta$  := height from free surface

$h$  := bathymetry height (rest + source)

$g$  := gravitational constant ( $9.8\text{m/s}^2$ )

$$\begin{cases} \frac{\partial H}{\partial t} + \nabla \cdot (H \mathbf{u}) = 0 \\ \frac{\partial (H \mathbf{u})}{\partial t} + \nabla \cdot (H \mathbf{u} \otimes \mathbf{u} + \frac{1}{2} g H^2) = g H \nabla h \end{cases}$$

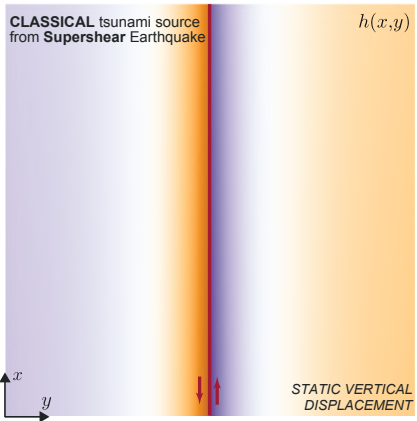


$$H = \eta(x, y, t) - h(x, y, t)$$

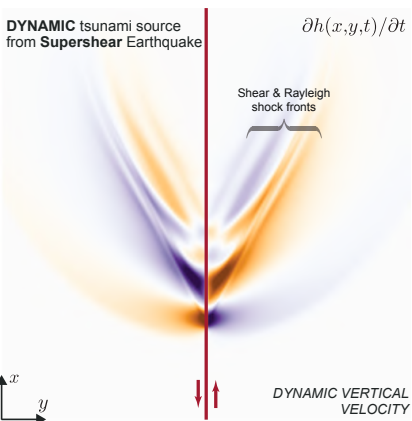
$$\frac{\partial H}{\partial t} = \frac{\partial \eta(x, y, t)}{\partial t} - \frac{\partial h(x, y, t)}{\partial t}$$

# Sourcing the tsunami

**Classical:**  $h(x, y, t) = h(x, y)$

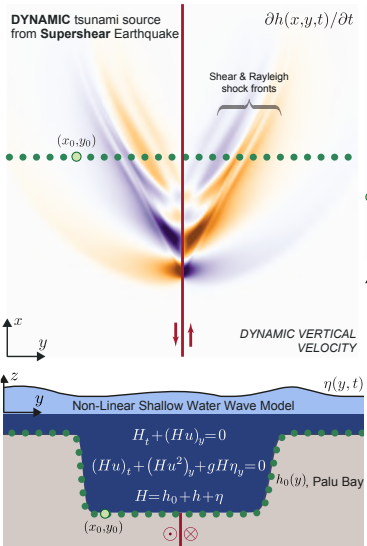
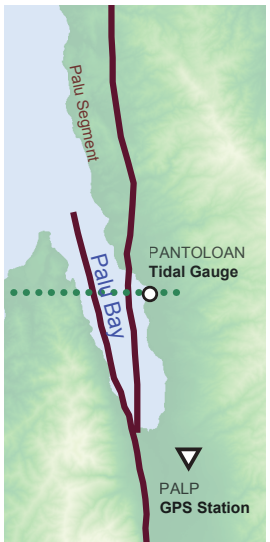


**Dynamic:**  $\partial h(x, y, t)/\partial t$  &  $h(x, y, t)$



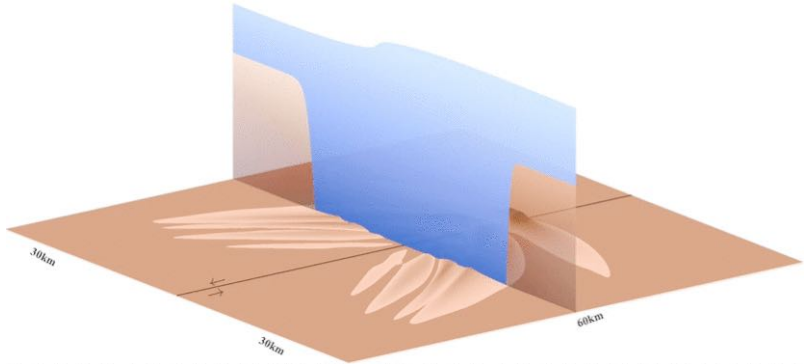
Amlani, et al., *Geophysical Journal International* (2022)

# FC-based modeling with the full supershear dynamics



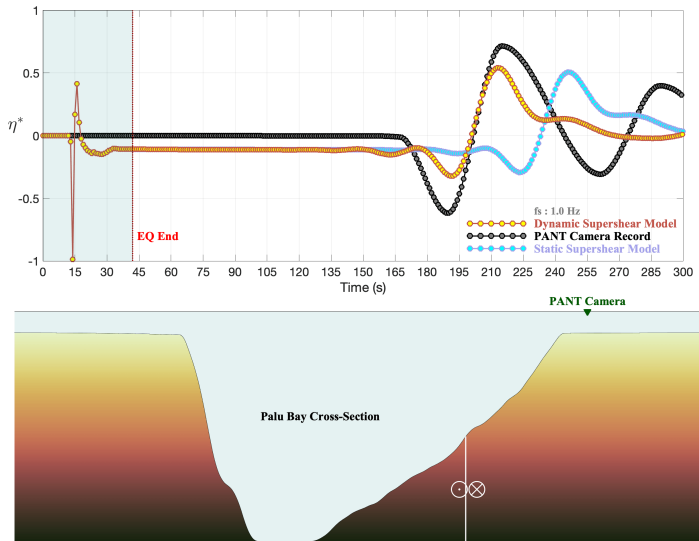
 Amlani, et al., *Geophysical Journal International* (2022)

# Coupling dynamic rupture & tsunami PDE solvers



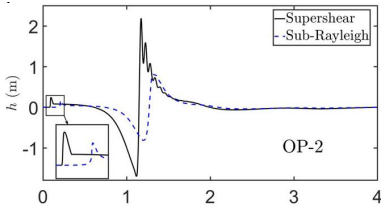
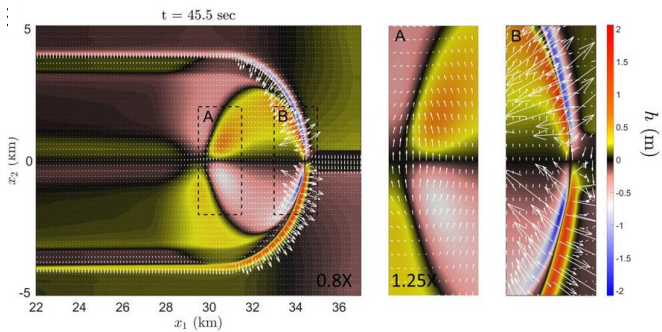
 Amlani, et al., *Geophysical Journal International* (2022)

# Capturing the arrival & first motions at Palu



 Amlani, et al., *Geophysical Journal International* (2022)

# Capturing wave heights in similar geometries



Elbanna, Abdelmeguid, Ma, Amlani, et al., *Proc Nat Acad Sci USA (PNAS)* (2021)

# Implications on tsunami risk for similar configurations

- ▶ supershear-capable **strike-slip** rupture + shallow bay

Izmit Bay, Turkey



Tomales Bay, California



SATELLITE IMAGE COURTESY M. RYMER, USGS

📘 Amlani, et al., *Geophysical Journal International* (2022)

📘 Elbanna, Abdelmeguid, Ma, Amlani, et al., *Proc Nat Acad Sci USA (PNAS)* (2021)

# Applications to cardiovascular hemodynamics

## Primary collaborator:

Niema M. Pahlevan (*fluids/biomechanics*,  University of Southern California)

## Clinical collaborator:

Kevin S. King (*neuroradiology*,  Barrow Neurological Institute)

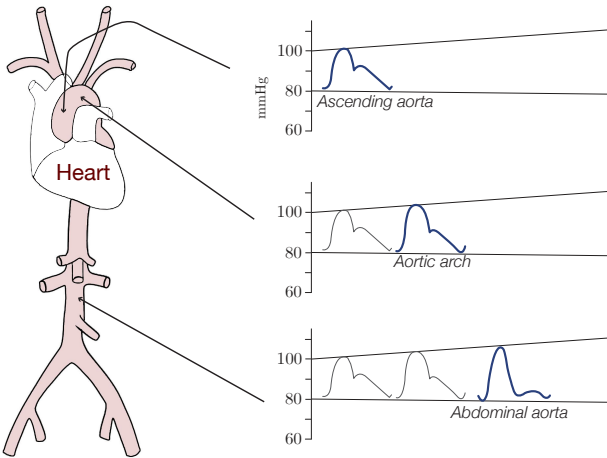
Some of the following was supported by:

U.S. **National Institutes of Health** (NIH Grant # 1-R56AG068630-01)

# Motivation

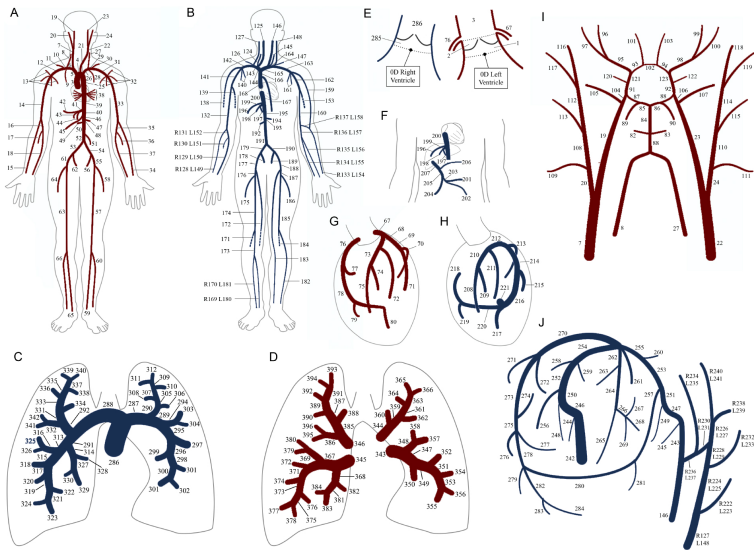
## ► arterial pulse waves in the human circulatory system

Segment pressure profiles



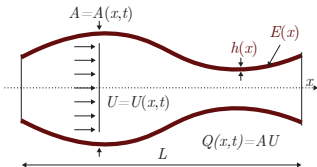
## The complete circulation (a closed loop)

**red**: systemic (forward); **blue**: pulmonary (return)

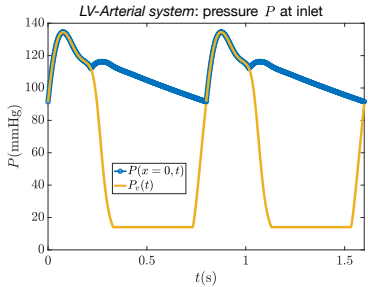


# Reduced-order models for hemodynamic wave propagation

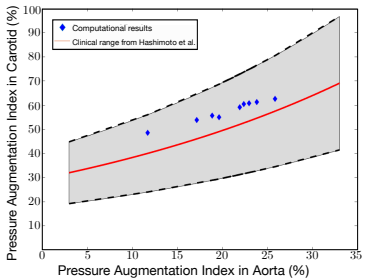
3D



Non-diseased valve



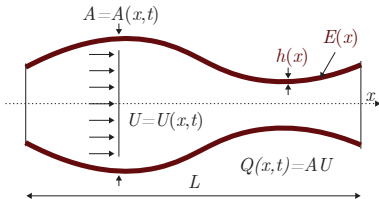
Comparisons to clinical data



Amlani & Pahlevan, Journal of Computational Physics (2020)

Aghilinejad, Amlani, et al., Scientific Reports (2020)

# Governing nonlinear fluid-structure PDE system



► 2D-axisymmetric **Navier-Stokes** in a segment (area  $A$ , velocity  $U$ , pressure  $P$ ):

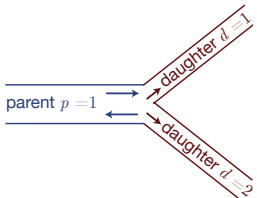
$$\begin{pmatrix} \frac{\partial A}{\partial t}(x, t) \\ \frac{\partial U}{\partial t}(x, t) \end{pmatrix} = - \begin{pmatrix} \frac{\partial(AU)}{\partial x}(x, t) \\ U \frac{\partial U}{\partial x}(x, t) + \frac{1}{\rho} \frac{\partial P}{\partial x}(x, t) + \frac{2(\zeta+2)\mu\pi U(x, t)}{\rho A(x, t)} \end{pmatrix}$$

► **nonlinear elastic tube law** (stiffness  $\beta$ , diastolic pressure & area  $P_d$  &  $A_d$ ):

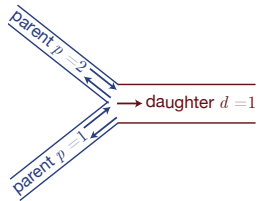
$$P(x, t) - P_{\text{ext}} = P_d + \beta(x) \left( \sqrt{A(x, t)} - \sqrt{A_d(x)} \right), \quad \beta(x) = \frac{4}{3A_d(x)} \sqrt{\pi} E(x) h(x)$$

# Vessel junctions & intersections

Diverging bifurcations (or trifurcations)



Merging bifurcations (or trifurcations)



► continuity of total pressure & conservation of mass at boundary:

$$P_p + \frac{\rho}{2} U_p^2 = P_d + \frac{\rho}{2} U_d, \quad p, d \in \mathbb{Z} \quad \text{&}$$

$$\sum_p A_p U_p = \sum_d A_d U_d$$

# Closing junction systems with characteristic equations

- quasi-linear form of governing PDEs in a segment:

$$\frac{\partial \mathbf{U}}{\partial t} + \mathbf{H} \frac{\partial \mathbf{U}}{\partial x} = \mathbf{F} \quad \text{s.t.} \quad \mathbf{U} = \begin{pmatrix} A \\ U \end{pmatrix}, \mathbf{H} = \begin{pmatrix} U & A \\ \frac{\beta}{2\rho\sqrt{A}} & U \end{pmatrix}, \mathbf{F} = -\frac{1}{\rho} \begin{pmatrix} 0 \\ 2(2+\zeta) \frac{\mu U}{A} + \frac{\partial P}{\partial x} \end{pmatrix}$$

- eigenvalues via  $|\Lambda I - \mathbf{H}| = 0 \iff \Lambda = \begin{pmatrix} \lambda_1 \\ \lambda_2 \end{pmatrix} = U \pm \sqrt{\frac{\beta\sqrt{A}}{2\rho}} = \boxed{\begin{pmatrix} U+c \\ U-c \end{pmatrix}}$

- left eigenvectors:

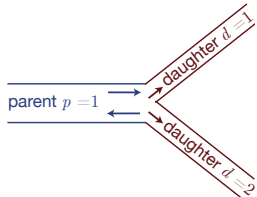
$$\boxed{\mathbf{L} = \begin{pmatrix} c/A & 1 \\ -c/A & 1 \end{pmatrix}}$$

- introduce characteristic variables via C.O.V. ( $\partial \mathbf{W}/\partial \mathbf{U} = \mathbf{L}$ )  $\implies$

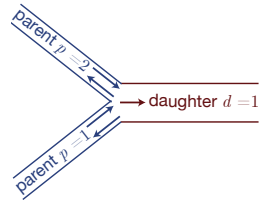
$$\frac{\partial \mathbf{W}}{\partial t} + \Lambda \frac{\partial \mathbf{W}}{\partial x} = \mathbf{0} \iff \boxed{W_{1,2} = U \pm 4(c - c_0) = U \pm 4\sqrt{\frac{\beta}{2\rho}} \left( A^{1/4} - A_0^{1/4} \right)}$$

# Closing junction systems with characteristic equations

Diverging bifurcations (or trifurcations)



Merging bifurcations (or trifurcations)



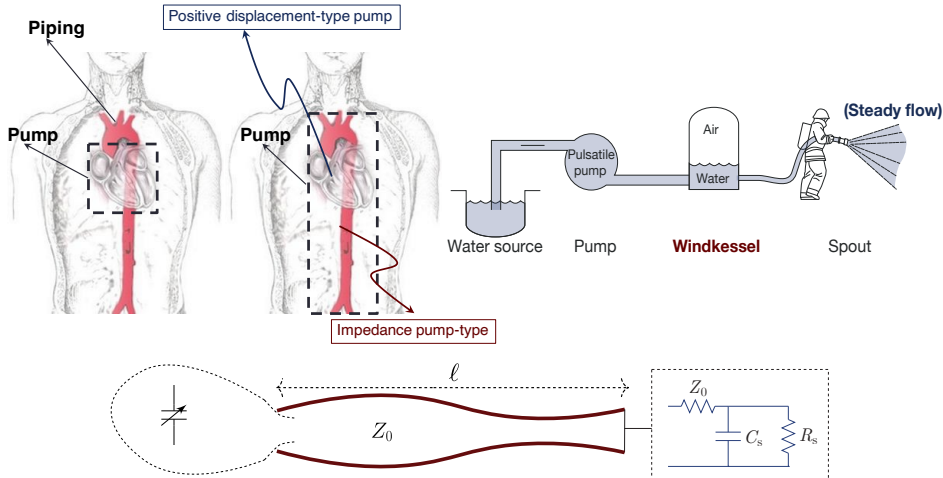
► continuity of total pressure & conservation of mass at boundary:

$$P_p + \frac{\rho}{2} U_p^2 = P_d + \frac{\rho}{2} U_d, \quad p, d \in \mathbb{Z} \quad \text{and} \quad \sum_p A_p U_p = \sum_d A_d U_d$$

► compatibility conditions of propagating characteristics:

$$w_{\text{forward},p} = U_p + 4A_p^{1/4} \sqrt{\frac{\beta_p}{2\rho}}, \quad w_{\text{backward},d} = U_d - 4A_d^{1/4} \sqrt{\frac{\beta_d}{2\rho}}, \quad p, d \in \mathbb{Z}$$

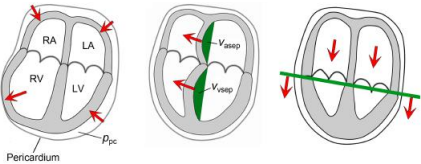
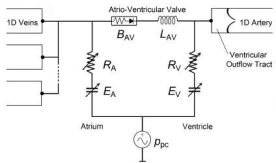
# Lumped parameter ODE models for microvasculature



$$\left\{ \begin{array}{l} \frac{\partial P_c}{\partial t}(t) = \frac{1}{C_s Z_0} P(x = \ell, t) - \frac{R_s + Z_0}{C_s R_s Z_0} P_c(t) \\ Q(x = \ell, t) = \frac{1}{Z_0} (P(x = \ell, t) - P_c(t)) \end{array} \right.$$

**load impedance**  
(arterial system)

# Elastance-based ODE models for heart chambers & valves



Nonlinear, non-stationary coupling

## Ventricular/Atrium

**valve is open (systole)**

$$\frac{dP_v}{dt} = -E_v(t) \left[ \frac{d}{dt} \left( \frac{1}{E_v} \right) P_v + Q_v(t) \right] + E^*(t) P^*(t)$$

**valve is closed (diastole)**

$$Q(t) = 0$$

## Aortic Valve

$$\Delta P(t) = \left( \rho / 2A_{\text{eff}}^2(t) \right) Q(t) |Q(t)| + (\rho L_{\text{eff}} / A_{\text{eff}}(t)) \frac{dQ}{dt}$$

$$A_{\text{eff}}(t) = [A_{\text{eff,max}}(t) - A_{\text{eff,min}}] \zeta(t) + A_{\text{eff,min}}$$

**valve opening**

$$\frac{d\zeta}{dt} = \zeta K_{\text{close}} \Delta P(t)$$

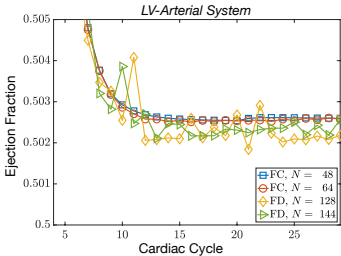
**valve closing**

$$\frac{d\zeta}{dt} = (1 - \zeta) K_{\text{open}} \Delta P(t)$$

Physiological relevance

## Ejection Fraction (EF)

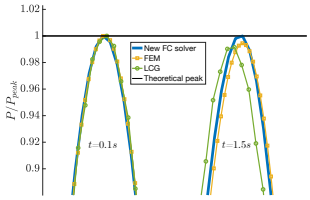
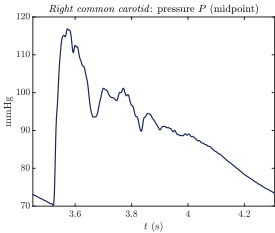
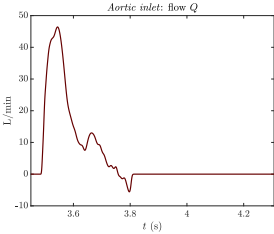
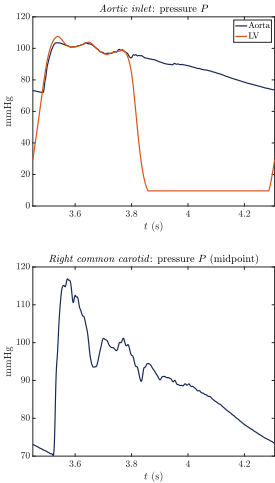
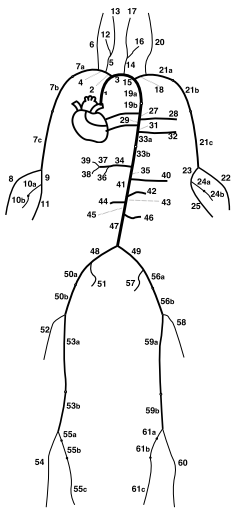
$$:= V^v(t) / V^* = \int_{T_{\text{per}}} Q(x_0, t) dt$$



Amlani & Pahlevan, *Journal of Computational Physics* (2020)

# Examples of FC-simulated waveforms

Heart Rate: 70 BPM; Cardiac Output: 5.5 L/min; healthy valve

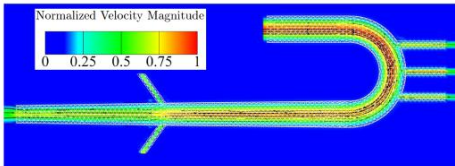
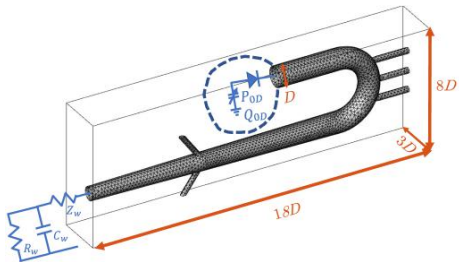
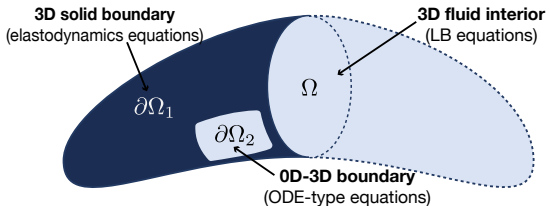


Amlani & Pahlevan, to be submitted (2023)

Amlani & Pahlevan, *Journal of Computational Physics* (2020)

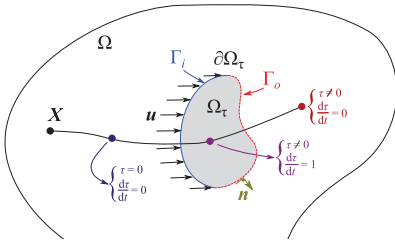
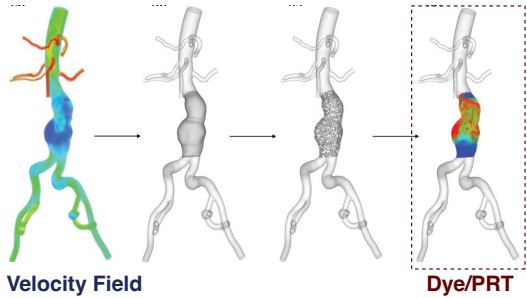
# Coupling 3D models with 0D/1D models

- ▶ studying non-Newtonian effects & therapeutic interventions



Wei, Amlani, Pahlevan, *Int. Journal of Numerical Methods in Biomedical Engineering* (2023)

# Dye evolution & particle residence times (PRT)



$$\frac{\partial \phi}{\partial t}(\mathbf{x}, t) + \mathbf{v}(\mathbf{x}, t) \cdot \nabla \phi(\mathbf{x}, t) - \nabla \cdot D(\mathbf{x}, t) \nabla \phi(\mathbf{x}, t) = f(\mathbf{x}, t), \quad \mathbf{x} \in \Omega, \quad t \geq 0$$

**Dye Concentration** ( $\phi(\mathbf{x}, t) := c(\mathbf{x}, t)$ ,  $f \equiv 0$ )

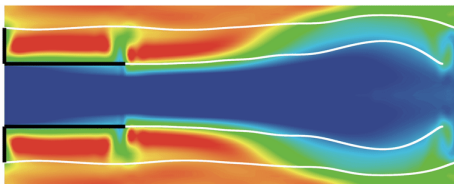
$$\begin{cases} \nabla c(\mathbf{x}, t) \cdot \mathbf{n} = 0, & \mathbf{x} \in \partial\Omega_N, \\ c(\mathbf{x}, t) = 1, & \mathbf{x} \in \Gamma_{\text{dye}} \subset \partial\Omega_D, \\ c(\mathbf{x}, t) = 0, & \mathbf{x} \in \partial\Omega_D \setminus \Gamma_{\text{dye}}, \end{cases}$$

**PRT** ( $\phi(\mathbf{x}, t) := \tau(\mathbf{x}, t)$ ,  $f \equiv 1$ )

$$\begin{cases} \nabla \tau(\mathbf{x}, t) \cdot \mathbf{n} = 0, & \mathbf{x} \in \partial\Omega_N \\ \tau(\mathbf{x}, t) = 0, & \mathbf{x} \in \partial\Omega_D, \end{cases}$$

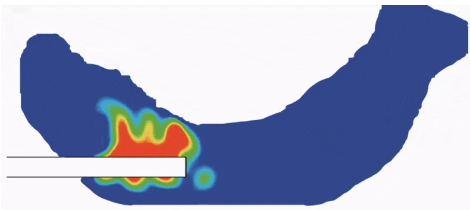
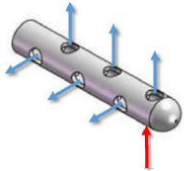
# Examples (velocity fields via a coupled lattice Boltzmann method)

- *aortic dissection*: FC-simulated **particle residence time**



- *catheter injection* ( $20^{\circ}\text{C}$ ): FC-simulated **dye evolution** ( $D(\mathbf{x}, t) \neq 0$ , supine position)

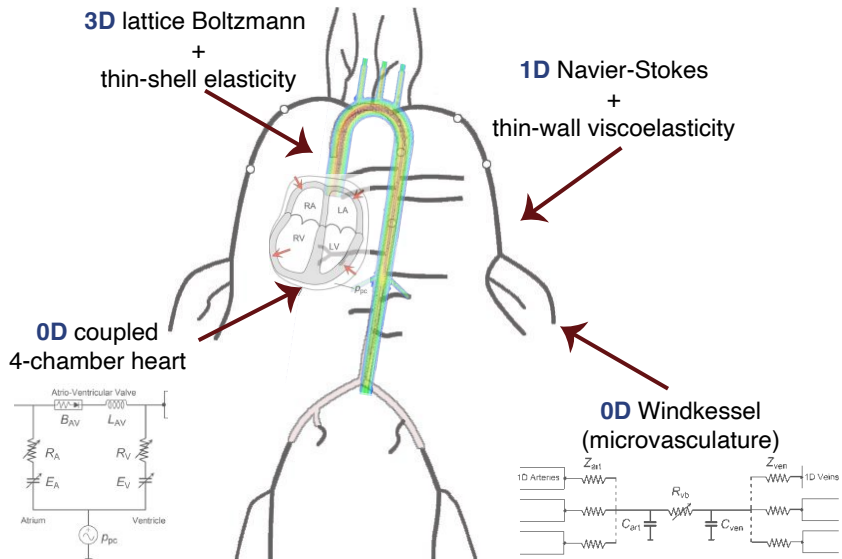
ILLUSTRATION OF THE CATHETER



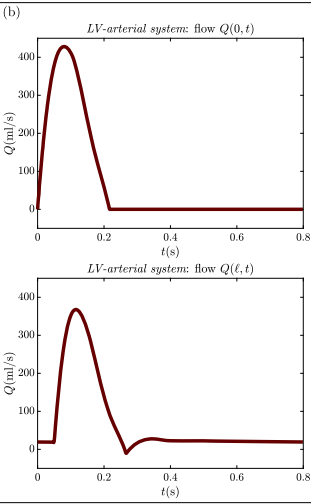
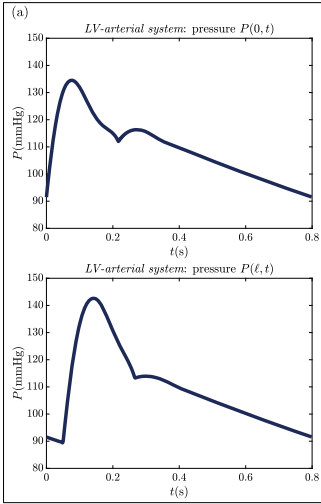
📄 [Amlani, et al., under review/arXiv:2112.05257 \(2023\)](#)

📄 [Bilgi, Amlani, et al., \*Annals of Biomedical Engineering\* \(2023\)](#)

# Towards more comprehensive multiscale modeling



# Hunting for clinically-relevant information in waveforms



E.g.

**Ejection Fraction (EF)**

$$\begin{aligned} &:= \frac{EDV - ESV}{EDV} \\ &= \int_{T_{per}} Q(0, t) dt \end{aligned}$$

**Pulsatile Power**

(mmHg mL/s)

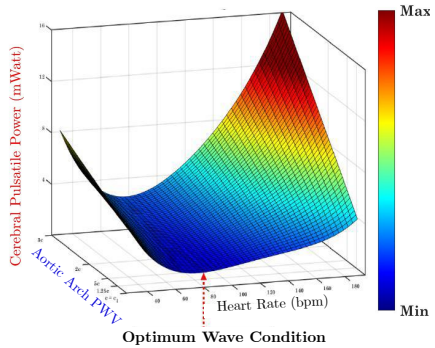
$$:= \int_{T_{per}} \frac{P(0, t)Q(0, t)}{T_{per}} dt$$

 Amlani & Pahlevan, *Journal of Computational Physics* (2020)

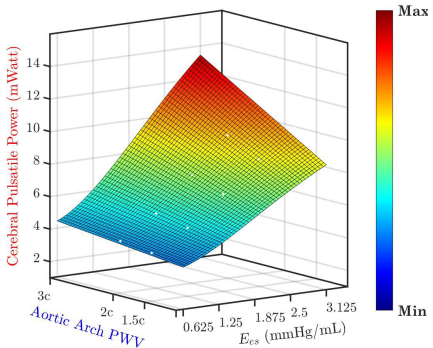
# Pulsatile energy to the brain

► clinically shown to be an indicator of dementia/Alzheimer's

As a function of **HR & aortic stiffness**



As a function of **contractility & stiffness**

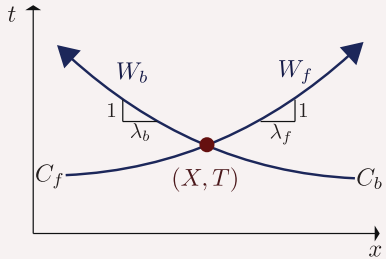
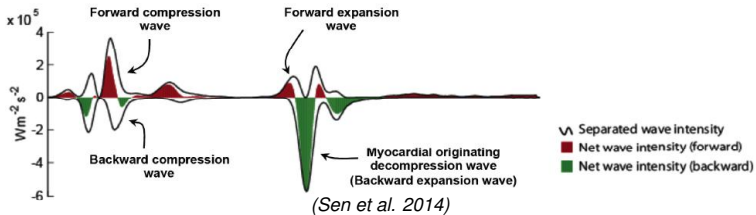


■ Aghilinejad, Amlani, et al., to be submitted (2023)

■ Aghilinejad, Amlani, et al., *Scientific Reports* (2020)

# Wave Intensity Analysis

- ▶ proposed by Parker & Jones (1990), inspired by methods for gas dynamics
- ▶ prognostic above standard risk factors (Koh 1998, De Silva 2012, Chisea 2019, ...)



Riemann invariants:

$$W_{f,b} = U \pm \int_{A_0}^A \frac{c(P)}{A} dA \quad \text{WI} \\ := dP(t) dU(t)$$

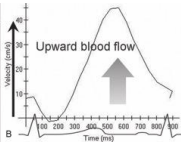
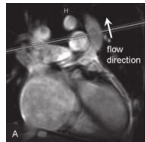
Characteristic paths:

$$C_{f,b} = \frac{dx_{f,b}}{dt} = U \pm c(P(A)) \\ = \frac{\rho c}{4} (dW_f^2 - dW_b^2)$$

# Pressure-only metrics for heart failure

► the **holy grail** for (cheap & easy) non-invasive diagnostics

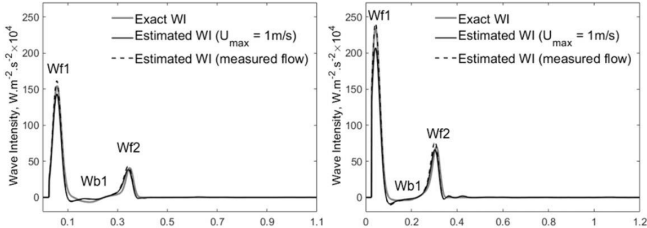
## Non-invasive flow (MRI)



## Non-invasive pressure

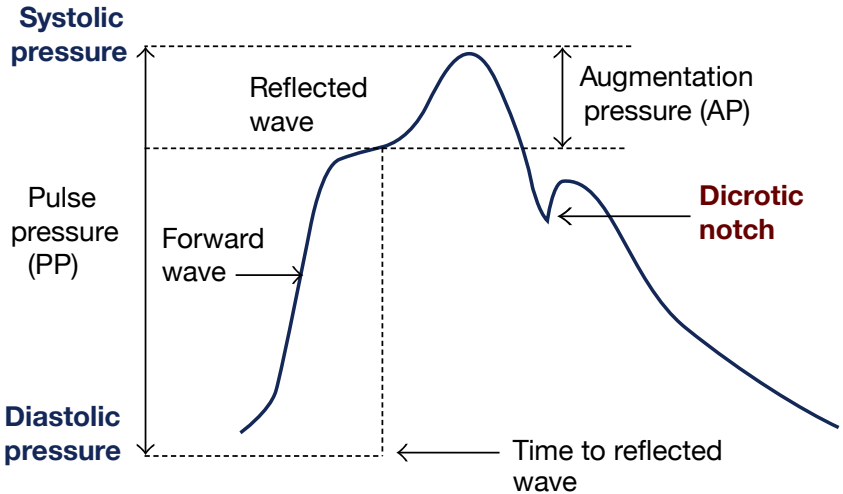


► **pressure-only estimates of WI (using a reservoir pressure approach):**



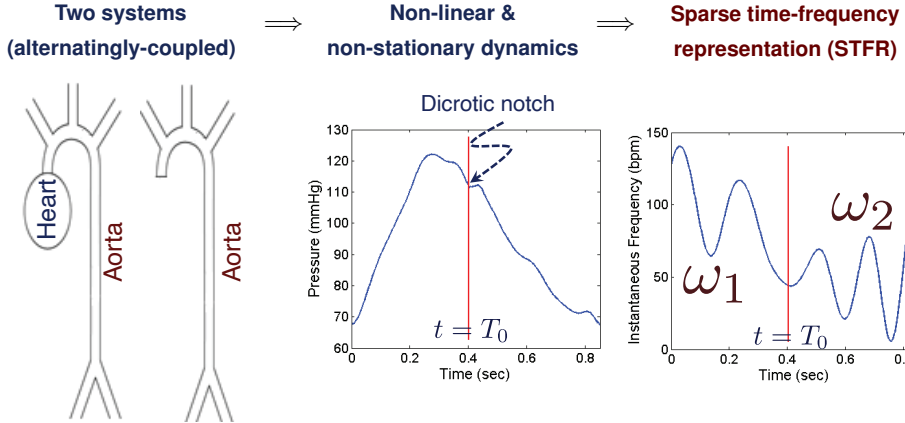
Aghilinejad, Amlani, et al., *Physiological Measurement* (2021)

# Analyzing signatures in waveform morphology

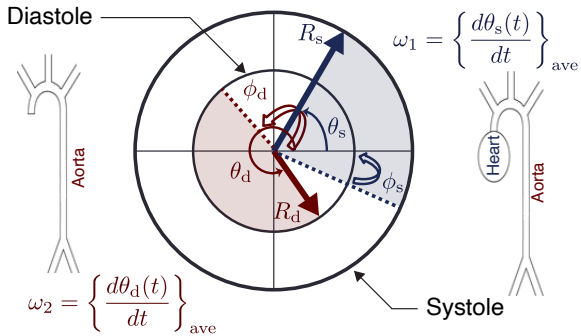


# The Intrinsic Frequency (IF) method

- introduced by Pahlevan et al. (2014), inspired by Hou & Shi (2011)
- Cooper et al. (2021): **IF parameters are biomarkers** that predict heart failure

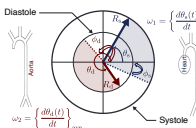


# IF: mathematical formulation



$$\begin{cases} \text{minimize: } & \|P(t) - \chi(t, 0, T_0)R_s \sin(\omega_1 t + \phi_1) - \chi(t, T_0, T)R_d \sin(\omega_2 t + \phi_2) - C\|_2^2 \\ & (\chi(t, t_0, t_1) := \mathbf{1}_{t_0 < t < t_1} \text{ is an indicator function}) \\ \text{subject to: } & \begin{cases} R_s(\omega_1 T_0 + \phi_1) = R_d(\omega_2 T_0 + \phi_2) & \text{(continuity)} \\ R_s(\phi_1) = R_d(\omega_2 T + \phi_2) & \text{(periodicity)} \end{cases} \end{cases}$$

# IF: computational challenges



$$\begin{cases} \text{minimize: } & \| P(t) - \chi(t, 0, T_0) R_s \sin(\omega_1 t + \phi_1) - \chi(t, T_0, T) R_d \sin(\omega_2 t + \phi_2) - C \|_2^2 \\ & (\chi(t, t_0, t_1) := \mathbf{1}_{t_0 < t < t_1} \text{ is an indicator function}) \\ \text{subject to: } & \begin{cases} R_s(\omega_1 T_0 + \phi_1) = R_d(\omega_2 T_0 + \phi_2) & \text{(continuity)} \\ R_s(\phi_1) = R_d(\omega_2 T + \phi_2) & \text{(periodicity)} \end{cases} \end{cases}$$

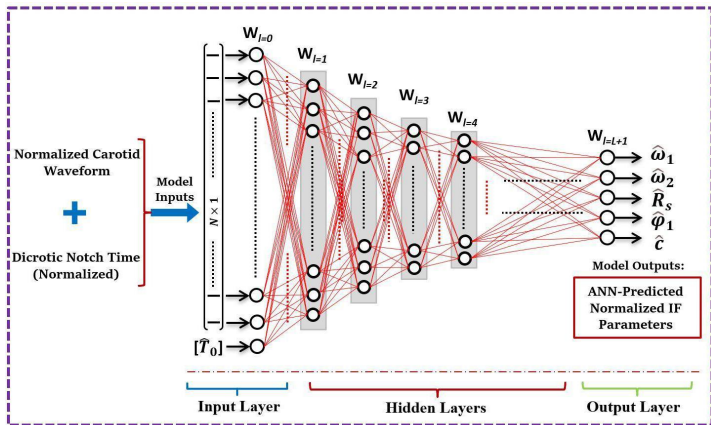
- ▶ fitting to discrete pressure data (e.g., of size  $N = 512$ )
- ▶ **multiple** optimization variables:

$$\begin{pmatrix} \omega_1 \\ \omega_2 \\ \phi_1 \\ \phi_2 \\ R_s \\ R_d \\ C \end{pmatrix} \in \mathbb{R}^7$$

- ▶ a **non-convex, non-linear** minimization problem (i.e., difficult & costly)

# Towards real-time diagnosis (prognosis?) of heart failure

- IF parameters scale across heterogeneous data (species, devices, real/synthetic)
- can use displacement as a surrogate (can show  $\omega_1^p/\omega_1^u \propto E_R/(1-g)$ )



Alavi, Dai, Amlani, Rinderknecht, et al., *Life Sciences* (2021)

Aghilinejad, ..., Amlani & Pahlevan, *Journal of Biomechanics* (2021)



**Call for PhD position:** high-order, high-fidelity modeling of tsunamis induced by dynamic earthquake motion

#### Supervisors

Dr. Faisal Amlani (*Université Paris-Saclay, CentraleSupélec, ENS Paris-Saclay, CNRS, LMPS, 91190, Gif-sur-Yvette, France*)

Dr. Harsha S. Bhat (*Laboratoire de Géologie, École Normale Supérieure, CNRS, PSL Research University, 75231, Paris, France*)

#### Advanced Modeling and Simulation in Engineering Sciences

[About](#)   [Articles](#)   [Submission Guidelines](#)

#### Open Topical Collections

Advanced Modeling and Simulation in Engineering Sciences welcomes collections on articles relating to an area of research formally decided upon by the Editorial team, within the scope of the journal and research community of advanced modeling and simulation of materials at large. The journal enthusiastically invites authors to submit their applicable work to our collections which have an ongoing call for papers.

Collections with ongoing calls for papers are listed below:

[Recent advances in Fourier-based computational approaches for PDEs](#)

Edited by: Faisal Amlani, Niema M. Pahlevan, Carlos Pérez-Arcibia



[Submit manuscript](#)

[Editorial Board](#)

[Sign up for article alerts and news from this journal](#)

[Follow](#)